BNXXXX-v0.0
September 22, 2025

Measurement of inclusive $B \to \Lambda_c$ branching fractions using Belle data and hadronic Full Event Interpretation

Leonardo Benjamin Rizzuto[1].

[1] *Institute Jožef Stefan, Ljubljana, Slovenia*

Abstract

Inclusive $B \to \Lambda_c$ branching fractions were measured most recently by BaBar collaboration. However, the measurement still presented a poor accuracy. A more precise measurement of inclusive $B \to \Lambda_c$ branching fraction could be useful to gain a better confidence on B meson weak decays treatment. With help of the Full Event Interpretation algorith, it is possible to perform a more precise measurment of inclusive $B \to \Lambda_c$ branching fractions using Belle data set.

Changelog

Version 1.0

Version for first review

- introduced the argumentation about the crossfeed ratio parametrization in Sec.**??**
- updated **??** in Sec.**??**, Table **??**, **??** and **??** (adjusting the comments)
- changed the linearity tests plots for charged correlated decays (**??** - **??** and Fig. 35 and Fig. 36 for anticorrelated decays)
- updated the systematics for chargeed correlated decays: summary Table **??**, **??** updated with the results from the 2D fit (having the crossfeed ratio param.), same for **??**. And for charged anticorrelated decays: summary Table 8 and Sections 6.8 -6.9.
- added the section about the systematics deriving from the parametrization of crossfeed normalization in the 2D fit (**??** and in charged anticorrelated decays Sec. 5.10), which takes into account the statistical uncertainties of the parameters.
- added the sections about the crossfeed peaking fraction in the 2D fit for anticorrelated decays (**??** and Sec. 5.11)
- Updated Table 7 for anticorrelated decays and also the corresponding plots.
- updated Table 12 for BR values of charged anticorrelated decays
- in the control sample chapter, updated Section 5.6 for the 2D fit on data, just adding the 2D fit performed on data using the parametrized normalization of crossfeed background, with results. And in the last section Sec. 4.13 added the new BR measured value for data.
- added Tracking efficiency to the systematics (see Sections 4.15 - 6.14)
- updated Sec. 4.13 for systematics on the control decay
- added Figures 51 , 52 and 53 in Appendix .2 relative to the optimized cuts discussed in Sec. 4.3
- corrected **??**

Contents

1 Introduction

Inclusive B meson baryonic decays with a Λ_c baryon in the final state are the most abundant, due to a relatively large V_{cb} element of the CKM matrix. The $BaBar$ experiment measured their branching fractions to be around the percent level (see ref. [1]). However, the branching fractions were determined with big uncertainties: nearly 50% on the measured values or, in the case of the $B^0 \to \Lambda_c^+$ decay, only an upper limit could be established. A more precise measurement of inclusive $B \to \Lambda_c$ branching fractions may shed light on the appropriateness of B meson weak decays treatment, particularly of strong interaction effects modelling. Predictions for inclusive branching fractions are given, for example, in ref. [2] or in [3] for $B \to \Lambda_c p$ decays.

Exploiting the Full Evenet Interpretation (FEI) algorithm, developed for the Belle II experiment, it may be possible to perform a more precise measurement of inclusive $B \to \Lambda_c$ branching fractions, using the full Belle data set. A more precise measurement may also trigger further research on currently scarce theory predictions for B meson decays to charm baryons.

1.1 Analysis Setup

The reconstruction is performed with `BASF2` release `05-02-03` together with the `b2bii` package in order to convert the *Belle* `MDST` files (`BASF` data format) to *Belle II* `MDST` files (`BASF2` data format). The FEI version used is `FEI_B2BII_light-2012-minos`.

1.2 Datasets

The Belle detector acquired a dataset of about $L_0 \approx 710 fb^{-1}$ of integrated luminosity in its lifetime at the $\Upsilon(4S)$ energy of 10.58 GeV, which corresponds to about 771 $\times 10^6 B\bar{B}$ meson pairs. Additionally, several streams of Monte-Carlo (MC) samples were produced, where each stream of MC corresponds to the same amount of data that was taken with the detector. No specific signal MC was used: instead of producing dedicated signal MC samples, the samples were obtained by filtering the decays of interest from the generic on-resonance MC samples. The following samples were used in this analysis:

- data
- MC - 10 streams of B^+B^- and $B^0\bar{B}^0$ (denoted as `charged` and `mixed`) for signal decays and backgrounds.
  - 6 streams of $q\bar{q}$ produced at $\Upsilon(4S)$ resonance energy
  - 6 streams of $q\bar{q}$ produced at 60 MeV below $\Upsilon(4S)$ resonance energy, where each stream corresponds to 1/10 $\times L_0$.

2 Event selection and reconstruction

In this chapter the procedure for reconstruction of the events where one B meson decays inclusively to a Λ_c baryon and the accompanying B meson decays hadronically.

2.1 B_{tag} reconstruction

The FEI is an exclusive tagging algorithm that uses machine learning to reconstruct B meson decay chains and calculates the probability that these decay chains correctly describe the true process. In this analysis only hadronically reconstructed decay chains are considered. The training called `FEI_B2BII_light-2012-minos` is used. Tag-side B meson candidates are required to have a beam-constrained mass greater than 5.22 GeV/c^2 and $-0.15 < \Delta E < 0.07$ GeV.
In the case of multiple candidates in the same event, the candidate with the highest SignalProbability (the signal probability calculated by FEI using FastBDT) is chosen. To suppress the background constisting of B^0 events misreconstructed as B^+ (and vice-versa) from neutral (charged) decays also a B^0 (B^+) candidate is reconstructed with FEI and if its SignalProbability is higher than the charged (neutral) reconstructed B meson, the event is discarded. This constitutes a sort of crossfeed-veto, rejecting part of events belonging to the other typology of decays of interest: for example in the case one is interested in reconstructing $B^{+/-}$ decays and the event actually contains $B^0/\bar{B}^0$ decays, the FEI reconstructed neutral B meson candidate most likely presents a higher SignalProbability than the charged FEI reconstructed candidate.

2.2 Λ_c reconstruction

In the *rest of event* (ROE) of the reconstructed B_{tag} meson, to select $\Lambda_c \to pK\pi$ signal candidates, the following event selection criteria are applied (same PID cuts were used for example in the Belle Note 1521 `https://belle.kek.jp/secured/belle_note/gn1521/BN_v1.pdf`). Charged tracks with the impact parameters perpendicular to and along the nominal interaction point (IP) are required to be less than 2 cm and 4 cm respectively ($dr < 2$ cm and $|dz| < 4$ cm).
The pion tracks are required to be identified with $\frac{\mathcal{L}_\pi}{\mathcal{L}_K+\mathcal{L}_\pi} > 0.6$. The kaon tracks are required to be identified with $\frac{\mathcal{L}_K}{\mathcal{L}_K+\mathcal{L}_\pi} > 0.6$, and the proton/anti-proton tracks are required to be identified with $\frac{\mathcal{L}_{p/\bar{p}}}{\mathcal{L}_K+\mathcal{L}_{p/\bar{p}}} > 0.6$ and $\frac{\mathcal{L}_{p/\bar{p}}}{\mathcal{L}_\pi+\mathcal{L}_{p/\bar{p}}} > 0.6$, where the $\mathcal{L}_{\pi,K,p/\bar{p}}$ are the likelihoods for pion, kaon, proton/anti-proton, respectively, determined using the ratio of the energy deposit in the ECL to the momentum measured in the SVD and CDC, the shower shape in the ECL, the matching between the position of charged track trajectory and the cluster position in the ECL, the hit information from the ACC and the dE/dx information in the CDC.
For the Λ_c candidates a vertex fit is performed with `TreeFitter`, requiring it to converge. If there are more than one Λ_c combination, then the best candidate based on the χ^2 probability is chosen. The Λ_c signal region is defined to be $|M_{\Lambda_c} - m_{\Lambda_c}| < 20$ MeV/c^2 ($\sim$

3σ), here m_{Λ_c} is the nominal mass of m_{Λ_c}.

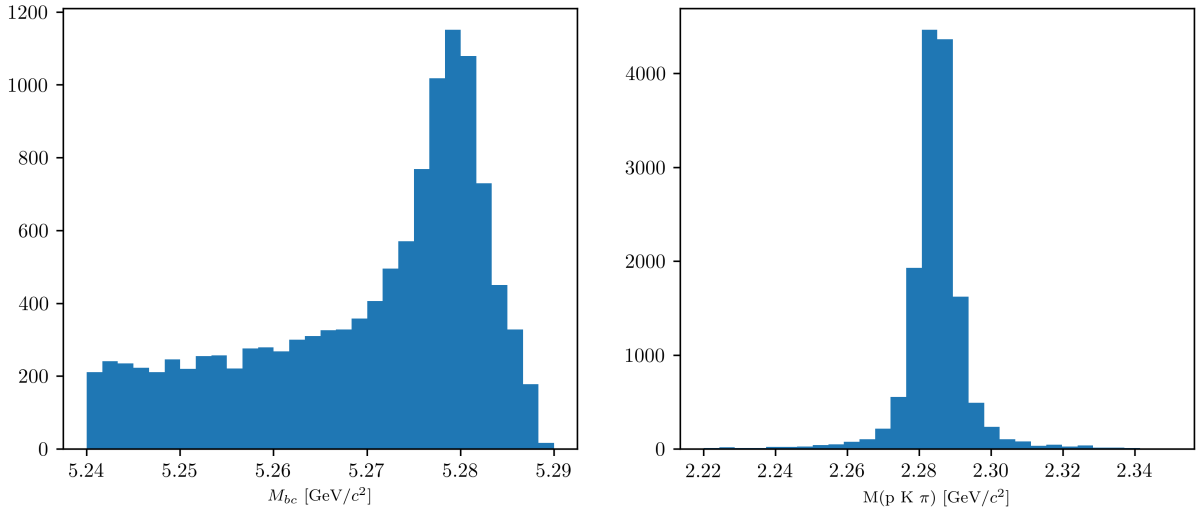

Figure (1) M_{bc} and $M(pK\pi)$ distributions of B_{tag} and Λ_c candidates reconstructed in the signal sample.

2.3 Wrongly reconstructed B_{tag} candidates

In the case of the signal sample the distributions for the beam-constrained mass M_{bc} and for the correctly reconstructed Λ_c candidates, look like in Fig. 1. If one then investigates the M_{bc} distribution of the B_{tag} candidates reconstructed with FEI, it can be seen that there is a peaking structure for wrongly reconstructed B mesons (as in Fig. 2), according to the BASF2 internal truth matching variable **isSignal**. It is obvious from this that the BASF2 internal truth matching variable cannot be used to separate properly the signal events in correctly and wrongly reconstructed B mesons. In the study BELLE2-NOTE-TE-2021-026 `https://docs.belle2.org/record/2711/files/BELLE2-NOTE-TE-2021-026.pdf` a possible solution was found developing new variables that can be used for an improved truth matching for the FEI (those variables were added to a newer BASF2 release than the one used for this study). In the present study instead a more "traditional" approach was adopted: fitting the M_{bc} distribution with a sum of PDFs that account for the flat (background) component and the peaking (signal) component. The first component represents the combinatorial background, i.e. B mesons that were mis-reconstructed, and therefore those events are denoted from now on as "**misreconstructed signal**". The peaking component represents the correctly reconstructed signal events in M_{bc} and therefore denoted from now on as "**reconstructed signal**". Only the second one is then considered for the signal yield, while the first is counted as a background. To validate this method a control decay study was performed on the flavor correlated $B^+ \to \bar{D}^0$ channel.

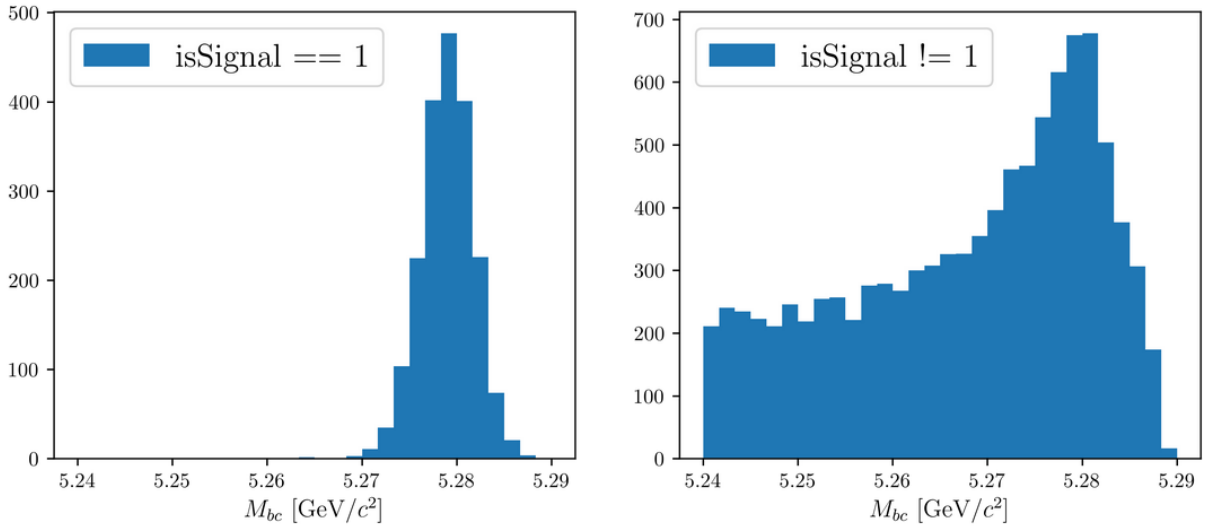

Figure (2) M_{bc} distribution of B_{tag} candidates reconstructed in the signal sample, truth-matched (on the left) and not (on the right).

3 Signal selection optimization

To further enhance the purity of the signal decays, an optimization procedure is adopted to determine optimal cuts for a set of variables for each decay mode under investigation by this study. The cuts on the following variables are optimized:

- $foxWolframR2$: the event based ratio of the 2-nd to the 0-th order Fox-Wolfram moments
- SignalProbability: the already mentioned signal probability calculated by FEI using FastBDT
- $p^{\Lambda_c}_{CMS}$: momentum of the Λ_c candidates in the center of mass system

The optimization is based on the Figure Of Merit (FOM): FOM $= \frac{S}{\sqrt{S+B}}$
Where S and B are respectively signal and background events in the signal region: $M_{bc} > 5.27$ GeV/c^2, $2.2665 < M(pK\pi) < 2.3065$ GeV/c^2.
Due to the issue reported in Sec. 2.3, to separate signal events that peak in M_{bc} from the ones that are not (which are then categorized as background events), the events reconstructed in the signal sample are fitted. with a sum of Crystal Ball function and Argus for each cut value on the corresponding variable to optimize (as in Fig. 3).

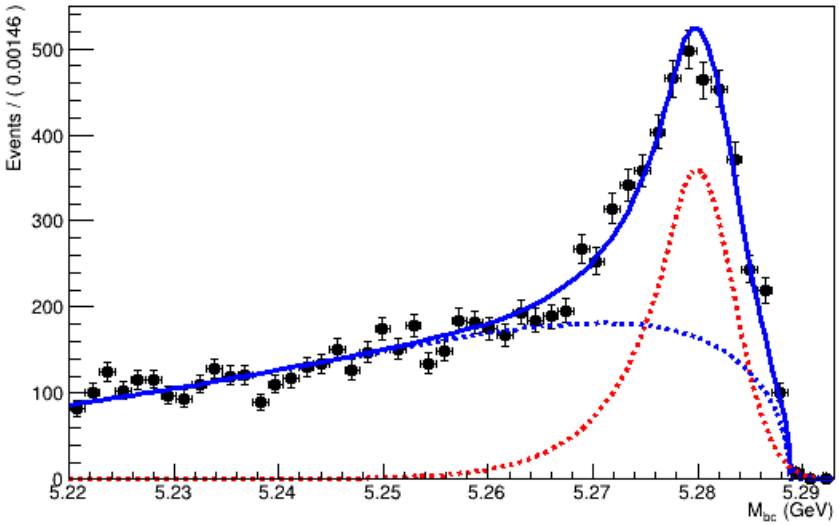

Figure (3) Example of a fit used to separate the correctly reconstructed B mesons (described by the red dotted Crystal Ball function) from the wrongly reconstructed ones (described by the blue dotted Argus function).

4 $B^- \to D^0$ control decay

To monitor the analysis steps, which are applied to both measured and simulated data, a control decay of the form

$$B^+ \to D^0 X,\ D^0 \to K^+\pi^-$$

is used. The statistics is much more abundant for this channel.

4.1 Dataset used

For this analysis the amount of data and Monte Carlo simulated data used was restricted to the SVD2 period: experiments ranging from 31 to 65. This choice was made to save processing time, anyway most of the $B\bar{B}$ meson pairs were produced in this range of experiments (620 $\times 10^6$ out of almost 800 $\times 10^6$).

4.2 Event selection and reconstruction

The approach used for the inclusive decays reconstruction is the same as for the $B \to \Lambda_c$ analysis. The same FEI training was used, though excluding the signal decay $D^0 \to K^+\pi^-$ from the decay chains used by the FEI to reconstruct the B_{tag}. Same preliminary selection criteria were applied to the tag-side B meson candidates as well.
In the *rest of event* (ROE) of the reconstructed B_{tag} meson, to select $D^0 \to K^+\pi^-$ signal candidates, the following event selection criteria are applied:

- $dr < 2$ cm and $|dz| < 4$ cm
- $\frac{\mathcal{L}_K}{\mathcal{L}_\mathcal{K}+\mathcal{L}_\pi} > 0.6$

For the D^0 candidates a vertex fit is performed with `TreeFitter`, requiring it to converge. If there are more than one D^0 combination, then the best candidate based on the χ^2 probability is chosen. The D^0 signal region is defined to be $|M_{D^0} - m_{D^0}| < 30$ MeV/c^2 ($\sim 3\sigma$), where m_{D^0} is the nominal mass of D^0.

4.3 Signal selection optimization

Following the same procedure as for the $B \to \Lambda_c$ analysis, the optimized selection cuts obtained for the event based ratio of the 2-nd to the 0-th order Fox-Wolfram moments, the B_{tag} signal probability and the momentum of the D^0 candidates in the center of mass system are[1]:

- $foxWolframR2 < 0.3$

[1] illustrative plots can be found in Appendix .2

- SignalProbability > 0.004
- $p^{D^0}_{CMS} > 1$ GeV/c^2

Figure 4 shows the distributions of M_{bc} and invariant mass in the signal region[2] for the $B^- \to D^0 X$ reconstructed events after the selection cuts were applied.

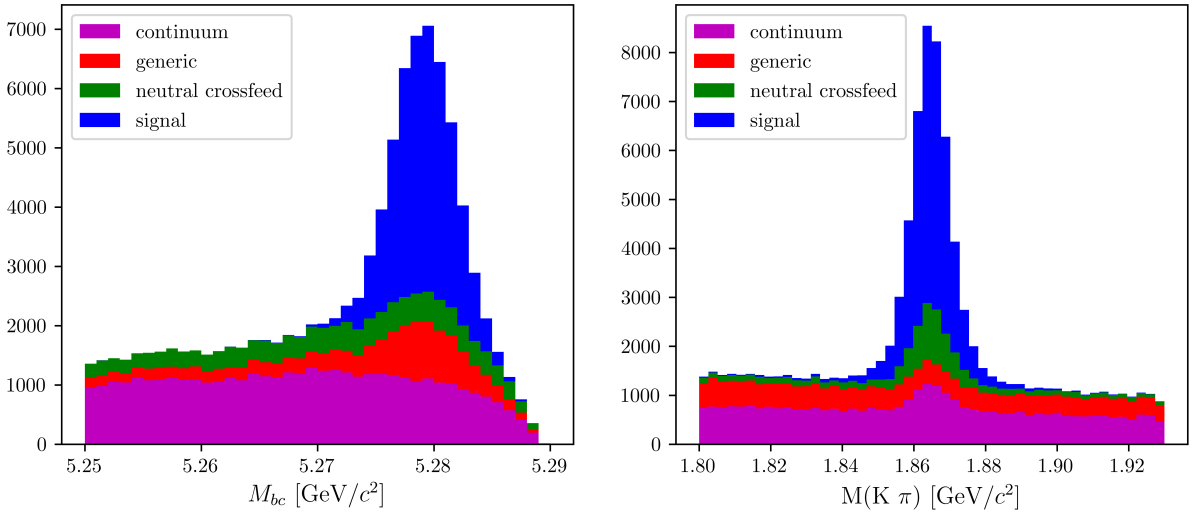

Figure (4) Distribution of M_{bc} (left) and invariant mass of charged correlated D^0 candidates (right), in the signal region after the above mentioned selection cuts.

4.4 Probability Density Functions (PDFs) for two dimensional fit

As already said the main goal of the control sample analysis is to ensure that the method used to extract the signal yields discriminating the correctly reconstructed from the misreconstructed signal events by fitting is valid. The reconstructed events in M_{bc} are fitted with a Crystal Ball, the misreconstructed signal with a Novosibirsk function. As in the $B \to \Lambda_c$ analysis both components have a correspondent peak in the D^0 mass which is fitted with a sum of three gaussians with a common mean. The fitted distribution of M_{bc} and $M(\pi K)$ are shown in Fig. 5 with signal MC sample.

[2]signal region: $M_{bc} > 5.27$ GeV/c^2 and $|M_{D^0} - m_{D^0}| < 30$ MeV/c^2

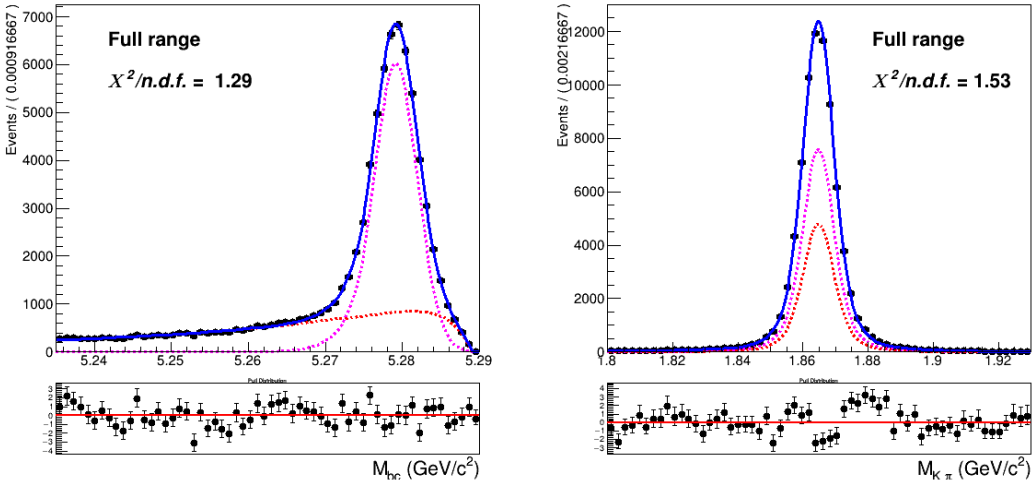

Figure (5) Two dimensional fit of total signal events in M_{bc} and $M(pK\pi)$ (in magenta reconstructed signal PDF, misreconstructed signal PDF in red)

As already seen in the $B \to \Lambda_c$ analysis besides the misreconstructed signal the other background components are:

- **generic** (charged B) background
- **crossfeed** (neutral B) background
- **continuum** background

Generic background

The generic background deriving from other B^+B^- events presents a similar shape in M_{bc}: it is fitted again with a sum of Crystal Ball and Novosibirsk function. Instead the distribution in the D^0 mass is fitted with a sum of first order Polynomial function and a small gaussian peak, which is due to the small amount of flavor anti-correlated $B^+ \to D^0$ reconstructed events (see Fig. 6). The total two-dimensional PDF is a product of the one-dimensional PDFs in M_{bc} and D^0 mass:

$$P^{GenBkg}_{B,D^0}(M_{bc}, M(K\pi)) = [\Gamma_{CB}(M_{bc}) + \Gamma_{Nov}(M_{bc})] \times [\rho_{pol1}(M(K\pi) + \rho_G(M(K\pi)) \quad (1)$$

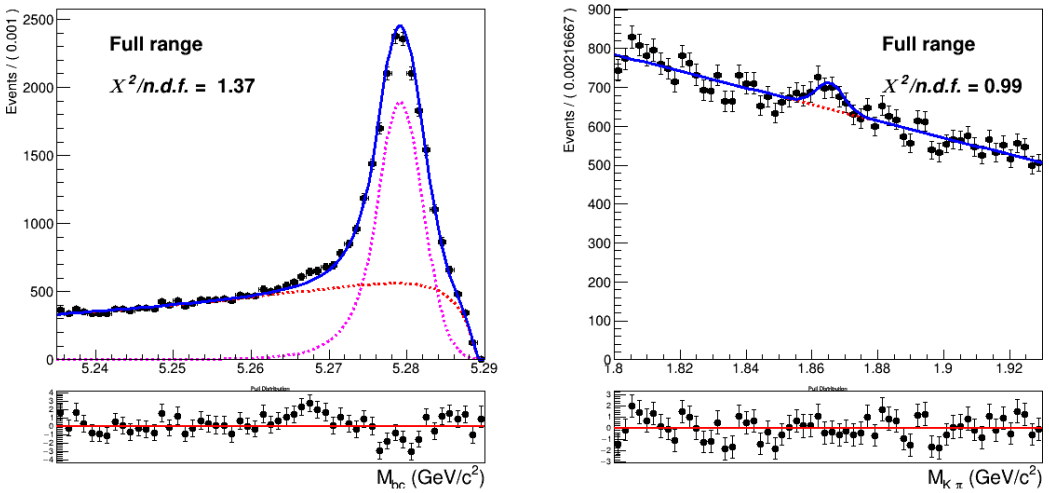

Figure (6) Two dimensional fit of generic (B^+B^-) background events in M_{bc} and $M(K\pi)$.

Crossfeed background The crossfeed background deriving from $B^0\bar{B}^0$ events is shown in Fig. 7 The M_{bc} distribution is fitted with a sum of Novosibirsk and Argus functions. The distribution in the D^0 mass is fitted with a first order Chebyshev polynomial and the D^0 mass peak is fitted with the same sum of three gaussians used to describe the signal peak (same parametrization used already in $B \to \Lambda_c$ analysis).

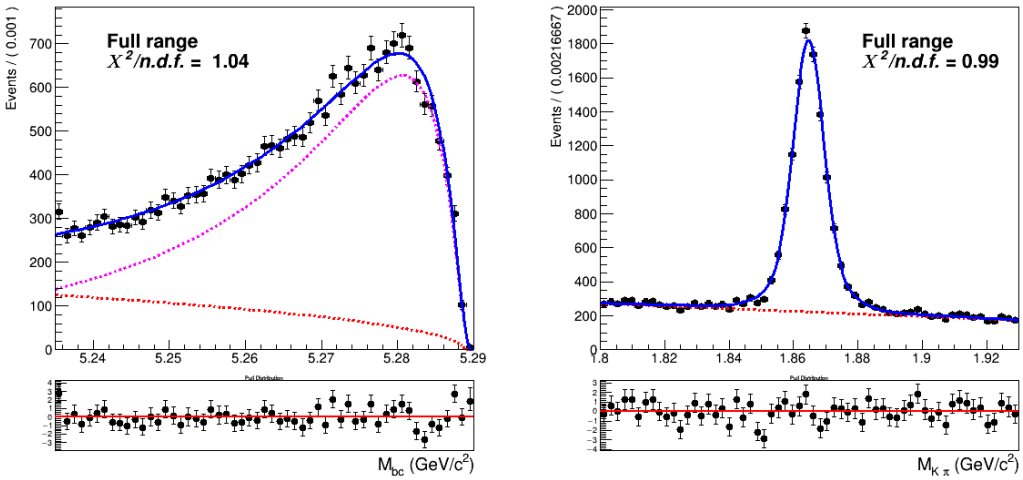

Figure (7) Two dimensional fit of crossfeed ($B^0\bar{B}^0$) events in M_{bc} and $M(K\pi)$.

Continuum background

The procedure adopted to model the continuum background is the same used for the $B \to \Lambda_c$ decays, but in this case the available statistics is enough to perform the scaling with all the selection cuts also in the case of the two-dimensional fit (not removing the continuum suppression).

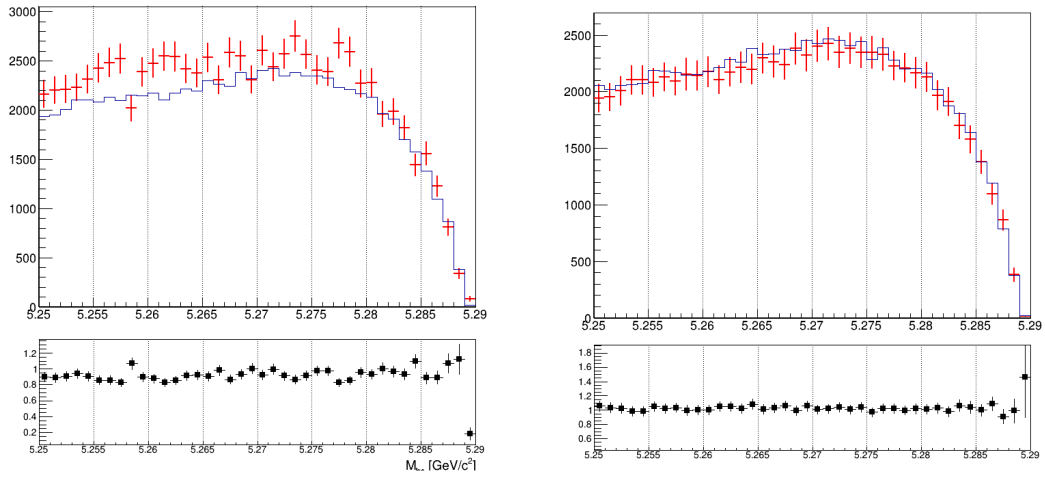

(a) (b)

Figure (8) In Fig. 8a M_{bc} distributions of the MC (scaled) off-resonance sample (in red) and on-resonance (in blue). In Fig. 8b M_{bc} distributions of the corrected scaled off-resonance and on-resonance MC continuum.

For each bin a correction factor is calculated, in order to have a reasonable match with the expected continuum background. Fig. 8b shows the applied correction on an independent MC sample. As in the case of $B \to \Lambda_c$ analysis, then the resulting M_{bc} distribution is fitted with a Novosibirsk function , whereas the D^0 mass distribution is fitted with a sum of first order Chebyshev polynomial and the sum of three gaussians used to describe the signal peak (as shown in Fig. 9). The fraction of events in the peak is the same in on- and off-resonance MC. This method is applied also to scale the off-resonance data.

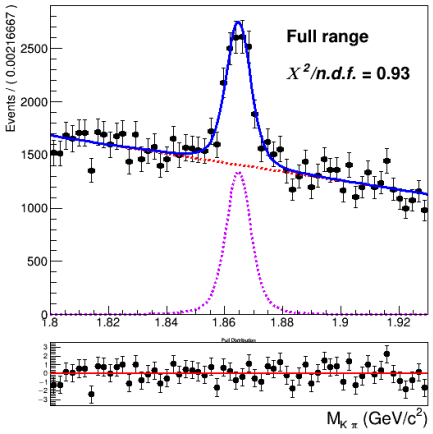

Figure (9) D^0 mass fit of scaled off-resonance Monte Carlo

4.5 2D Fit on Monte Carlo simulated data

As in the $B \to \Lambda_c$ study, five streams of Monte Carlo simulated data have been used to get values for the shaping parameters for the individidual components described in the previous section and the fit model is tested on an independent stream.

For the six fits, the same conditions were applied to the widths:

- σ_{G1}: the width of the wider of the three Gaussian functions in $\rho_G(M(K\pi))$
- σ_{CB} parameter for the Crystal Ball describing the signal
- the σ_{CB} parameter for the Crystal Ball describing the generic background is expressed as function of the signal σ_{CB} with a ratio fixed from the MC.

For the fits on Monte Carlo simulated data the crossfeed normalization is expressed as ratio of its contribution and the misreconstructed signal as found in MC and kept fixed (to see how the parametrized form impacts a fit on data is then performed). Exemplary, the distributions of stream 0 overlaid by the fitted PDF are depicted in Fig. 10 (see Appendix .2 for the projections of signal regions and sidebands).

In Table 1 the yields for reconstructed and misreconstructed signal are listed for each stream.

stream	0	1	2	3	4	5
NrecSig	56986 ± 400	57766 ± 437	55607 ± 426	57068 ± 372	58385 ± 369	57501 ± 437
NmisSig	31453 ± 321	30513 ± 350	32580 ± 350	33340 ± 399	29966 ± 390	32012 ± 355

Table (1) reconstructed and misreconstructed signal yields obtained fitting 6 independent streams

To be sure that the PDFs enables us to extract the signal yield in an unbiased way, the sum of reconstructed and misreconstructed signal yields, i.e. total signal, from the fits are compared to the true values of each stream (Table 2). There are quite some differences between the fitted signal yield and the true values in individual streams. However, all these deviations are within statistical expectations.

streams	fit	MC truth	fit - MC truth	
stream 0	88439 ± 340	88144	+ 295	(+0.33%)
stream 1	88279 ± 361	88551	−272	(- 0.31%)
stream 2	88187 ± 360	88487	-300	(- 0.34%)
stream 3	90408 ± 372	90149	+ 259	(+ 0.29%)
stream 4	88351 ± 383	87981	+ 370	(+ 0.42%)
stream 5	89513 ± 366	89710	-197	(- 0.22%)
sum	533177	533022	+155	(+0.03%)

Table (2) Comparison of fitted and truth-matched total signal events in each stream.

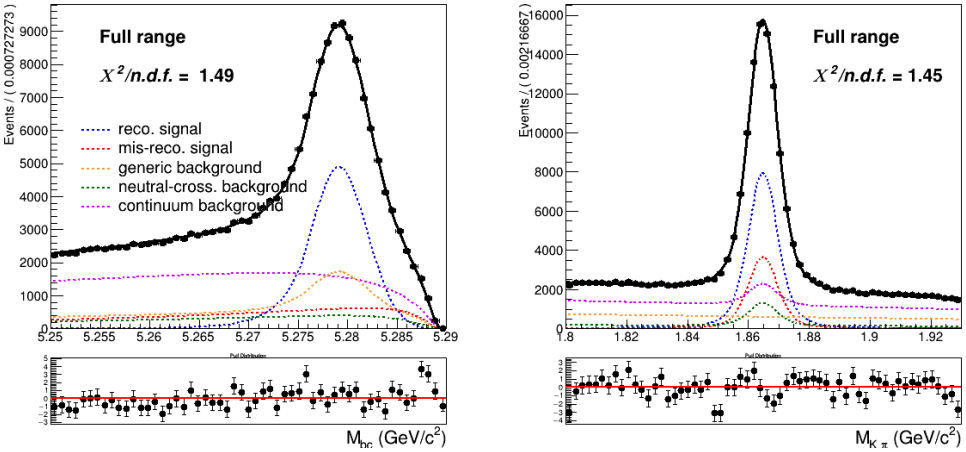

Figure (10) Two dimensional fit on stream 0 Monte Carlo simulated data.

4.6 2D Fit on data

After obtaining the model for the continuum background scaling and correcting the M_{bc} distribution of the off-resonance data, the model tested on Monte Carlo simulated data is applied on data with same free parameters and yields. Fig. 11 shows the projections of the two dimensional fit (see Appendix .2 for the projections of signal regions and sidebands). Yields for the reconstructed and misreconstructed signal and for generic background are obtained from the fit:

.

NrecSig	35629 ± 368
NmisSig	24425 ± 311
Generic	24596 ± 407

The total normalization from the fit is 174230 ± 407 (to be compared with the total data events: 173964).

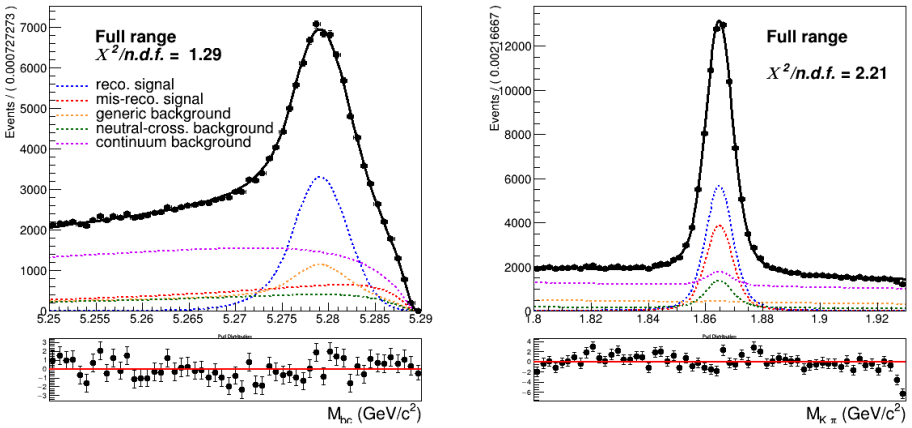

Figure (11) Two dimensional fit on Data (same conditions applied as in Fig. 10)

ratio	MC	DATA
NmisSig/NrecSig	0.56 ± 0.01	0.68 ± 0.01
NmisSig/Generic	0.90 ± 0.02	0.99 ± 0.02
Generic/NrecSig	0.62 ± 0.01	0.69 ± 0.02

Table (3) Comparison of ratios of yields from the two dimensional fits on Monte Carlo simulated data and on Data.

Since in the case of the two dimensional fit for the measurement of $B^- \to \Lambda_c^+ X$ decays the crossfeed normalization was parametrized in the form described by **??**, the 2D fit shown above is repeated with the parametrized normalization for the crossfeed background. The signal reconstruction efficiency that enters the formula to estimate the true number of signal events ($N_{sig} = N_{recSig}/\epsilon$) is now the signal reconstruction efficiency on data: ϵ_{data}. It can be estimated scaling the one found on Monte Carlo by a correction factor that takes into account the different FEI efficiency on data and the signal-side reconstruction corrected for the different PID efficiency (see Sec. 4.10-Sec. 4.11), $\epsilon_{data} = \epsilon_{MC} \cdot c_{FEI} \cdot c_{D^0} = (0.216 \pm 0.016)\%$.

where $c_{FEI} = 0.810^{+0.013}_{-0.012} \pm 0.054$ is the correction factor for the FEI efficiency determined in [5]
whereas the factor c_{D^0} is the PID correction reported in Sec. 4.10.
Fig. 12 shows this second fit.

ratio	MC	DATA
NmisSig/NrecSig	0.56 ± 0.01	0.66 ± 0.01
NmisSig/Generic	0.90 ± 0.02	0.93 ± 0.02
Generic/NrecSig	0.62 ± 0.01	0.71 ± 0.02

Table (4) Comparison of ratios of yields from the two dimensional fits on Monte Carlo simulated data and on Data (from the fit shown in Fig. 12).

In the following table yields for the reconstructed and misreconstructed signal and for generic background obtained from this second fit are reported:

NrecSig	36553 ± 360
NmisSig	24115 ± 283
Generic	25900 ± 409

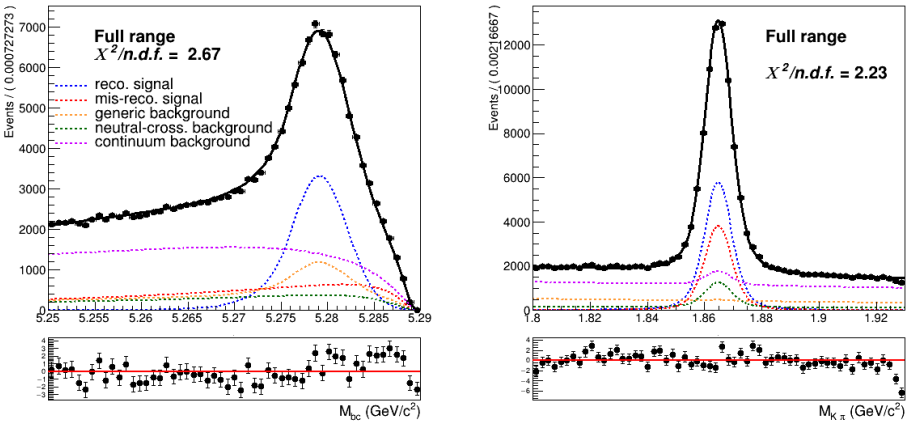

Figure (12) Two dimensional fit on Data with parametrized normalization of crossfeed background

4.7 Probability Density Functions (PDFs) for the B_{tag}

Like for the signal model in the 2D fit the M_{bc} distribution of the tagged charged B mesons is fitted with a Crystal Ball as for the reconstructed signal component, whereas the misreconstructed signal component is fitted with a Novosibirsk function (Fig. 13a).

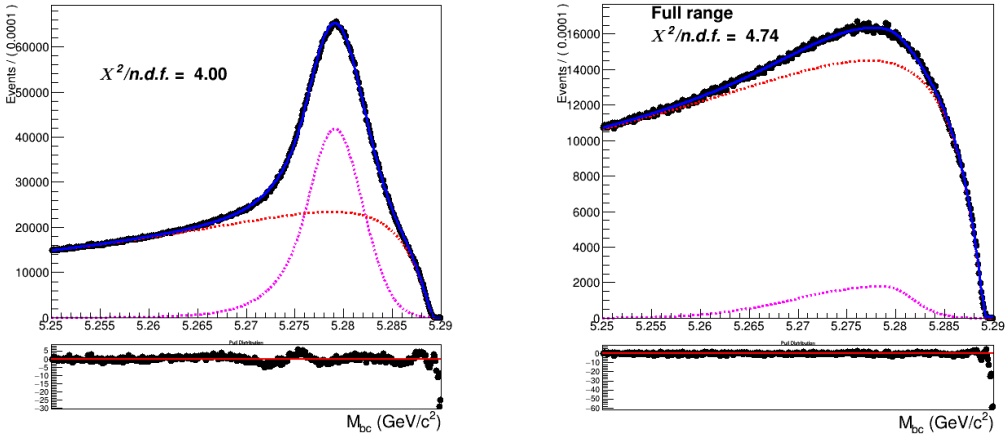

(a) (b)

Figure (13) On the left: fitted distribution of tagged charged B mesons, reconstructed signal events (magenta) are described by a Crystal Ball whereas the misreconstructed signal events (red) are described by a Novosibirsk function. On the right: Crossfeed distribution fitted with a sum of Novosibirsk (red) and asymmetric Gaussian PDF (magenta)

The crossfeed background is fitted instead with a sum of a Novosibirsk and an asymmetric Gaussian PDF (Fig. 13b).

Regarding the continuum background component, same procedure used for the 2D fit was applied to the M_{bc} distribution of the continuum background in this case (see Fig. **??** for the result).

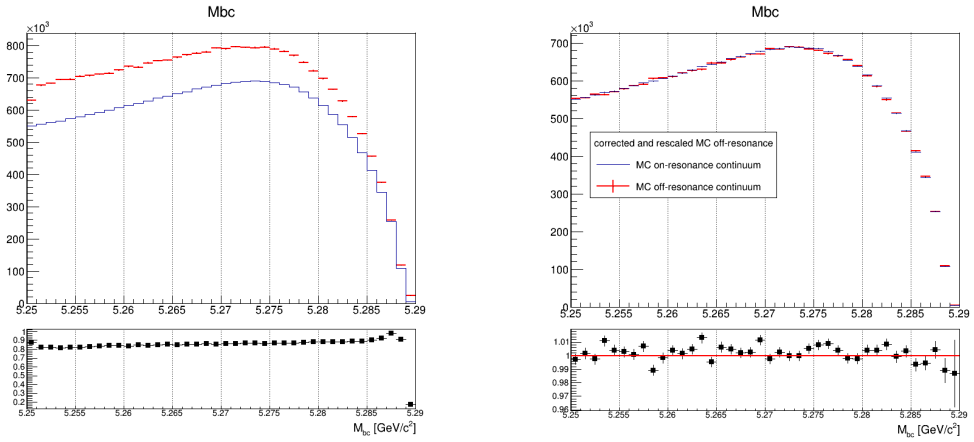

Figure (14) On the left: M_{bc} distributions of the MC off-resonance sample and the MC continuum sample. On the right: M_{bc} distributions of the corrected scaled MC off-resonance and on-resonance MC continuum.

4.8 B_{tag} Fit on Monte Carlo simulated data

An independent Monte Carlo stream was used to test the total fit model on tagged B mesons candidates. The usual condition is applied to the crossfeed background events: the ratio between its contribution and misreconstructed signal events is fixed from the other Monte Carlo stream.

In this fit the shaping parameters that are not kept fixed are the Crystal Ball width (σ_{CB}) and the width of the Novosibirsk function describing the misreconstructed signal events. As in the case of B_{tag} fit in Sec. **??** the range for the fit is restricted to values betweeen 5.250 and 5.287 GeV/c^2.

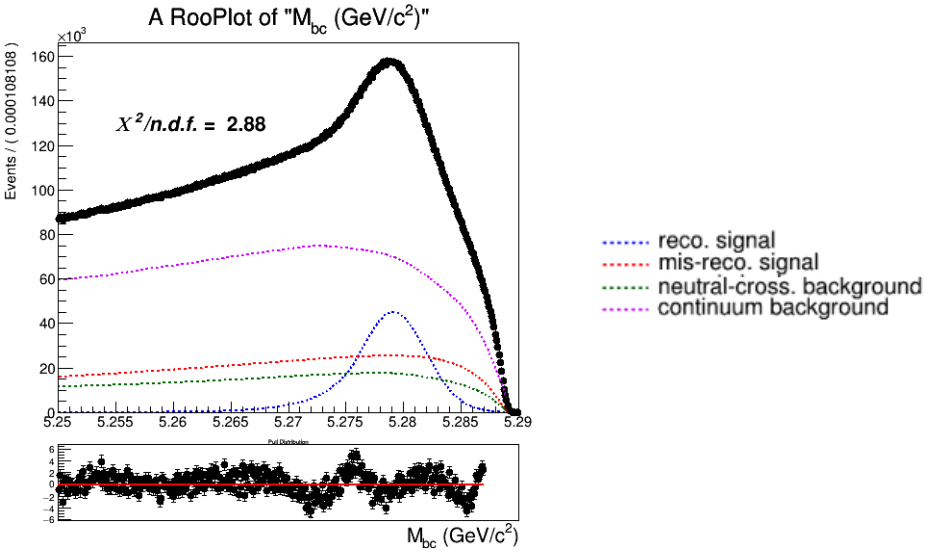

Figure (15) Total fit of tagged B mesons

Yields for the reconstructed and misreconstructed signal are obtained from the fit:

NrecSig	$3.25110 \cdot 10^6 \pm 6759$
NmisSig	$7.41107 \cdot 10^6 \pm 5341$

One can then compare the sum NrecSig+NmisSig (the so called total signal) with the true value known from the Monte Carlo and the same for the total number of events in this particular stream:

	fit	MC value
Total Signal	$10.662 \cdot 10^6 \pm 5249$	$10.671 \cdot 10^6$
Total events	$38.601 \cdot 10^6 \pm 6886$	$38.610 \cdot 10^6$

The discrepancy in the total signal events from the fit and the MC here is about 1.7σ, but the relative error is an order of magnitude smaller than the one found in B_{tag} fit in **??** (below the ‰level), therefore it's negligible.

4.9 B_{tag} Fit on data

The fit model tested on Monte Carlo simulated data is then applied with the same method on data Fig. 16.

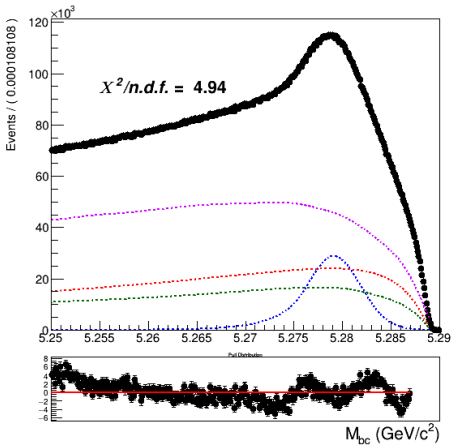

Figure (16) Total fit of tagged B^+ mesons candidates on data

Yields for the reconstructed and misreconstructed signal are obtained from the fit:

NrecSig	2.011·10 ^{6}± 5858
NmisSig	6.975·10 ^{6}± 4667
Total Signal	8.982·10 ^{6}±4587

ratio	MC	DATA
NmisSig/NrecSig	2.28 ± 0.01	3.47 ± 0.01

Table (5) Comparison of ratios of yields from the tagged B mesons fits on Monte Carlo simulated data and on Data.

4.10 PID efficiency correction

The PID selection is applied only to Kaons: $\frac{\mathcal{L}_K}{\mathcal{L}_K+\mathcal{L}_\pi} > 0.6$

Using the values provided in the global tag `BellePID` (as done in the $B \to \Lambda_c$ study), the average Kaon ID correction for this analysis is estimated to be $R = 0.976 \pm 0.008$.

4.11 D^0 and FEI efficiency

The efficiency in reconstructing the D^0 after correctly tagging the charged B meson, can be estimated from the 2D fit on Monte Carlo simulated data, using the reconstructed signal yield and from a sample of B_{tag} candidates reconstructed in signal events in the Monte Carlo: where from B^+B^- at least a D^0 decaying into πK is produced.

For the latter a fit is performed to extract the yield of correctly tagged B mesons (Fig. 17)

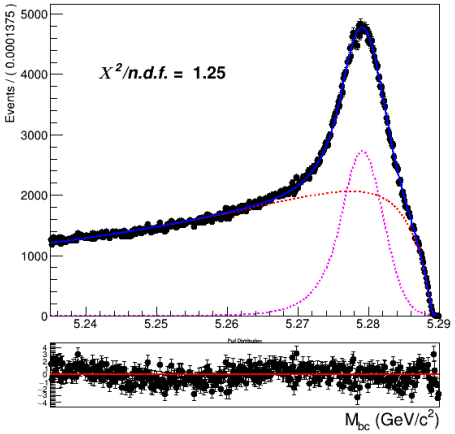

Figure (17) Fit of tagged B mesons in the "signal events" sample

Yields for the reconstructed and misreconstructed signal :

NrecSig	1.46779·10 ^{5}± 767
NmisSig	6.16717·10 ^{5}± 1028

From this and the results listed in Sec. 4.5 the efficiency to reconstruct D^0 is obtained :

$$\epsilon_{D^0} = \frac{NrecSig(2D)}{NrecSig((B^{sig}_{tag}} = 39.1 \pm 0.4\%^3 \qquad \text{(KID efficiency corrected value for data: 38.2 \%)}$$

The results from the fit shown in (Fig. 17) can be used also to calculate the FEI tag-side efficiency for signal events, i.e. the efficiency to tag the B meson accompanying a B_{sig} decaying into a D^0 on the signal side. Whereas results from the fit of charged B_{tag} shown

[3] the error reflects the limited Monte Carlo statistics

in Fig. 13a can be used to calculate the hadronic tag-side efficiency in the generic B^+B^- events case.
The ratio of the two efficiencies is found to be: $\frac{\epsilon^+_{FEI,sig}}{\epsilon^+_{FEI}} = 1.50 \pm 0.01$

4.12 Studies of Systematic Effects

The systematic uncertainties are studied the same way as in the case of the $B^+ \to \bar{\Lambda}_c^- X$ branching fraction. The values are reported in the next section. The dominant systematic uncertainty is the one originated by the continuum background modeling and its incidence in terms of relative error on the branching fraction value is same as for the $B^+ \to \bar{\Lambda}_c^- X$ study. For this control sample study the uncertainty that would be caused by the uncertainty of the crossfeed peaking events is not estimated, since the uncertainty on $\mathcal{B}(B^0 \to \bar{D}^0 + X)$ is only of few percent and the possible effect can be considered negligible compared to the other systeamtic uncertainties.

4.13 Measured $B^+ \to \bar{D}^0 X$ inclusive Branching Fraction

The inclusive branching fraction of $B^+ \to \bar{D}^0 X$ can be determined by:

$$Br(B^+ \to \bar{D}^0) = \frac{r}{Br(D^0 \to K^+\pi^-)\epsilon_{D^0}} \cdot \frac{\epsilon^+_{FEI}}{\epsilon^+_{FEI,sig}} \tag{2}$$

Where

- $r = \frac{N_{tag,D^0}}{N_{tag}}$ is the ratio of reconstructed signal yield in the two dimensional fit and in the M_{bc} fit of the tagged B mesons.
- ϵ_{D^0} is the D^0 reconstruction efficiency calculated as fraction of reconstructed signal events with correct tag of which then also a correctly reconstructed D^0 is reconstructed in the signal side.
- $\frac{\epsilon^+_{FEI}}{\epsilon^+_{FEI,sig}}$ is the ratio of the FEI efficiencies: the hadronic tag-side efficiency for generic B^+B^- events (ϵ^+_{FEI}) and signal-side depedent one ($\epsilon^+_{FEI,sig}$) where one of the two B mesons decays inclusively into the signal channel ($D^0 \to K^+\pi^-$)
- $Br(D^0 \to K^+\pi^-) = 3.8\%$ in Belle DECAY.DEC table, $Br(D^0 \to K^+\pi^-) = 3.95\%$ in PDG.

In Monte Carlo: $Br(B^+ \to \bar{D}^0) = 79.4 \pm 0.6^{(stat.)}\%$ (true MC value: 79.1%)

As for the Data, the value obtained using a fixed ratio of crossfeed events with respect to misreconstructed signal events is: $Br(B^+ \to \bar{D}^0) = 78.3 \pm 0.8^{(stat.)}\%$

While, introducing the parametrization of the crossfeed normalization in the two dimensional fit gives a larger value: $Br(B^+ \to \bar{D}^0) = 80.3 \pm 0.8^{(stat.)}\%$
Nevertheless, the latter is in agreement with the value reported by the PDG: $(79 \pm 4)\%$

One can conclude that the obtained results have proven the validity of the method chosen for the measurements.

The systematic uncertainties are dominating as one can see from the Table below, listing the contribution of the various sources of systematics in terms of Branching Fraction in percentage.

continuum modelling	1.8 %
Crossfeed PFDs	0.4 %
Crossfeed fraction	0.8 %
2DFit crossfeed normalization	0.4 %
FEI efficiency	0.5 %
ϵ_{D^0}	0.8 %
PID	0.6 %
Tracking efficiency	0.8 %
Total	2.5 %

Table (6) Sources of systematic uncertainties and their contributions.

5 $B^- \to \bar{\Lambda}_c^-$ decays

Applying the same procedure already illustrated in **??**, the optimized selection cuts for the charged flavor-anticorrelated decays are:

- $foxWolframR2 < 0.3$
- SignalProbability > 0.1
- $p_{CMS}^{\Lambda_c} < 1.5$ GeV/c

5.1 Probability Density Functions (PDFs) for the two dimensional fit

The PDFs used to describe the signal distributions are the same already used in **??** (only the shaping parameters differ) and an example of the 2D fit is shown in Fig. 18. Also the generic background deriving from other B^+B^- events presents similar shapes of the distributions as shown already in **??**, therefore the probability density functions used are the same (fit is shown in Fig. 19).

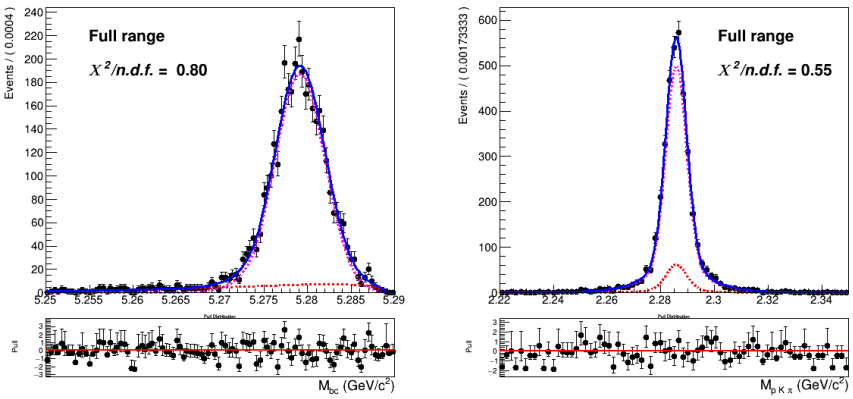

Figure (18) Two dimensional fit of total signal events in M_{bc} and $M(pK\pi)$.

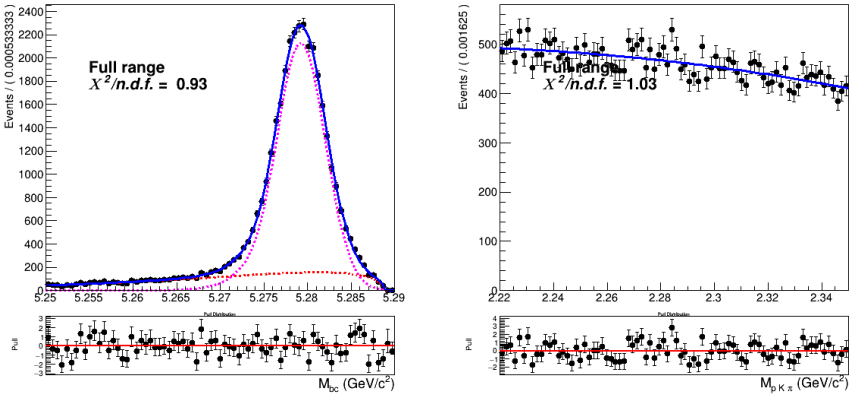

Figure (19) Two dimensional fit of generic (B^+B^-) events in M_{bc} and $M(pK\pi)$.

The same can be said about the misreconstructed B^0 events (Fig. 20)

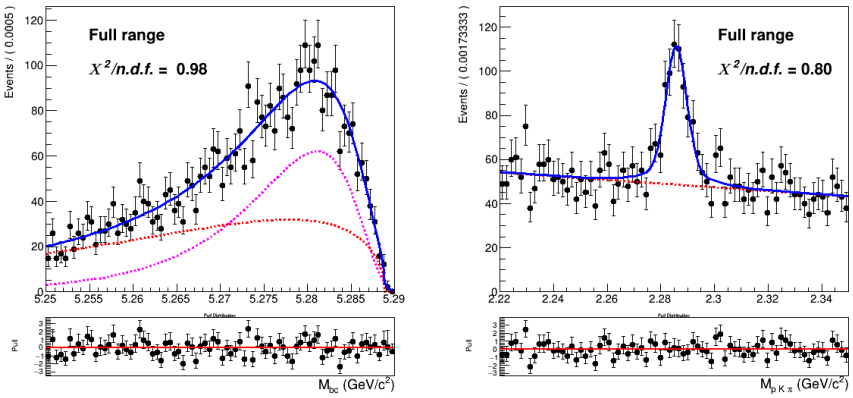

Figure (20) Two dimensional fit of crossfeed ($B^0\bar{B}^0$) events in M_{bc} and $M(pK\pi)$.

To check that the shapes determined using 5 streams of Monte Carlo are describing with reasonable accuracy the 2D distribution, the projections of the fit of the two-dimensional distributions in the signal and sideband regions are plotted (Fig. 22 - Fig. 24). One can see the same tendencies of undershooting/overshooting the Λ_c invariant mass peak, as in the case of charged correlated decays (Figures **??** - **??**). But when examining the independent Monte Carlo stream distribution overlaid by the determined PDF in the very same regions (see Figures 25 -27) those effects are so much diminished, according to the statistics, that the effects are within statistical fluctuations and therefore negligible, contrary to the case of charged flavor-correlated decays.

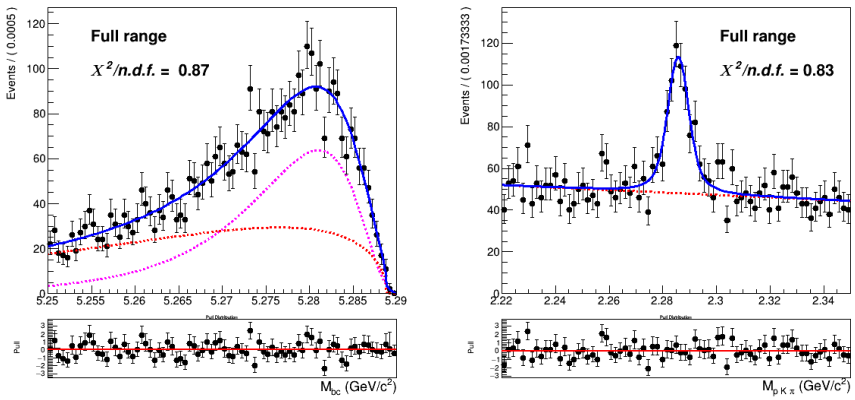

Figure (21) Two dimensional fit of crossfeed ($B^0\bar{B}^0$) events in M_{bc} and $M(pK\pi)$.

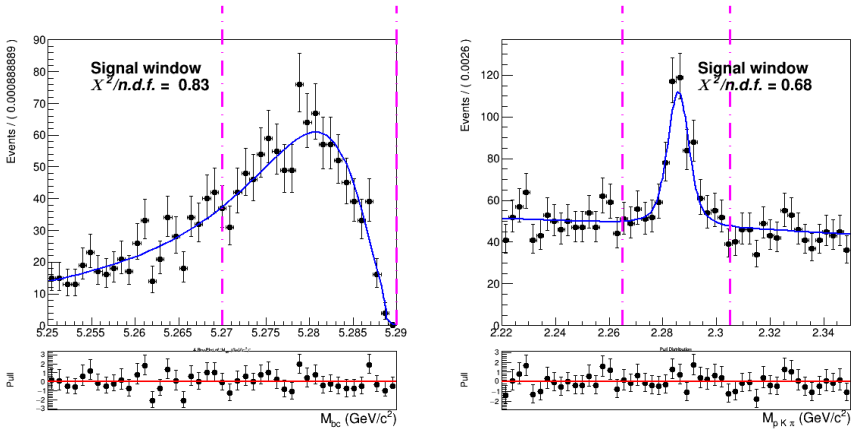

Figure (22) Signal region projections in M_{bc} and $M(pK\pi)$ of the fit of crossfeed events.

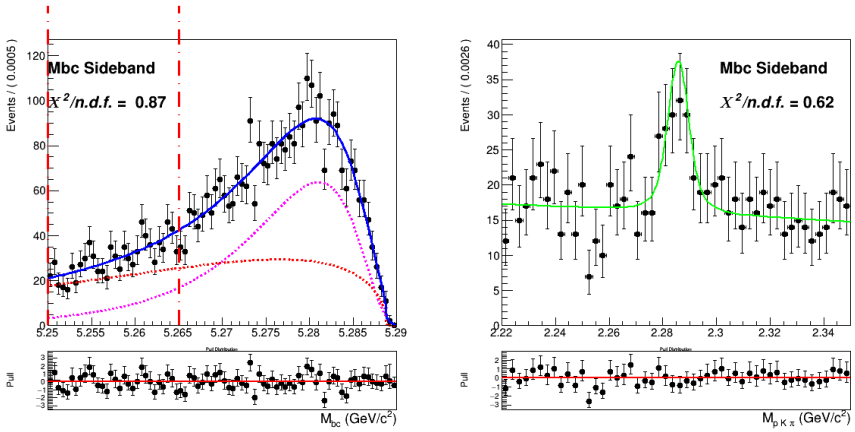

Figure (23) M_{bc} sideband region projection of the fit of crossfeed events in $M(pK\pi)$.

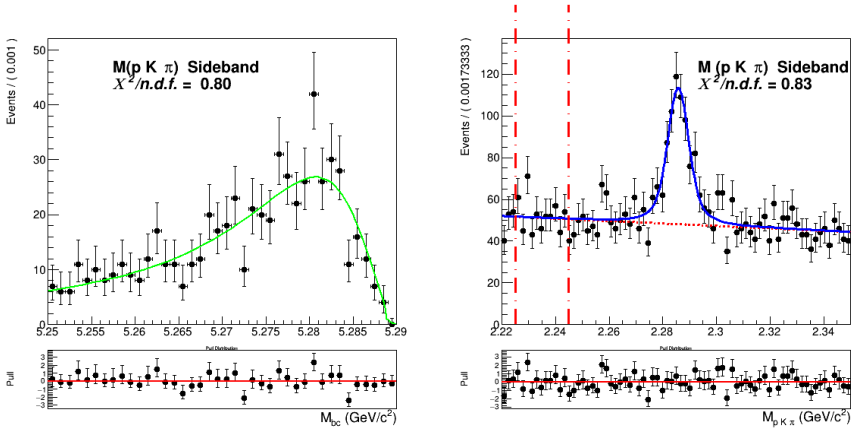

Figure (24) $M(pK\pi)$ sideband region projection of the fit of crossfeed events in M_{bc}.

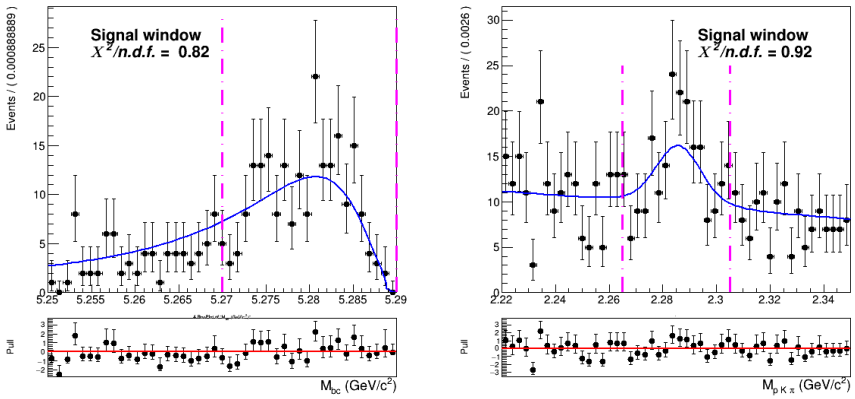

Figure (25) Signal region projections in M_{bc} and $M(pK\pi)$ of the fit of crossfeed events.

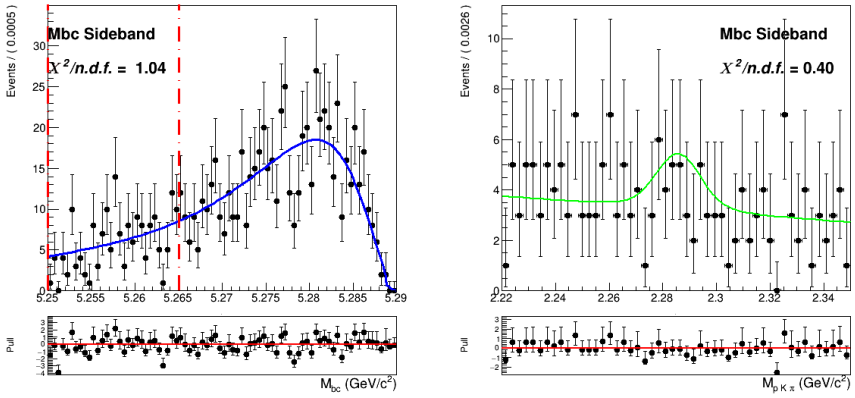

Figure (26) Two dimensional fit of crossfeed ($B^0\bar{B}^0$) events in M_{bc} and $M(pK\pi)$.

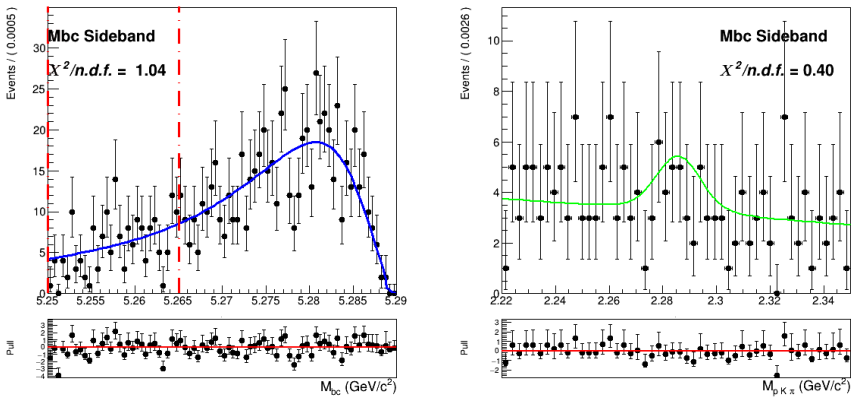

Figure (27) Two dimensional fit of crossfeed ($B^0\bar{B}^0$) events in M_{bc} and $M(pK\pi)$.

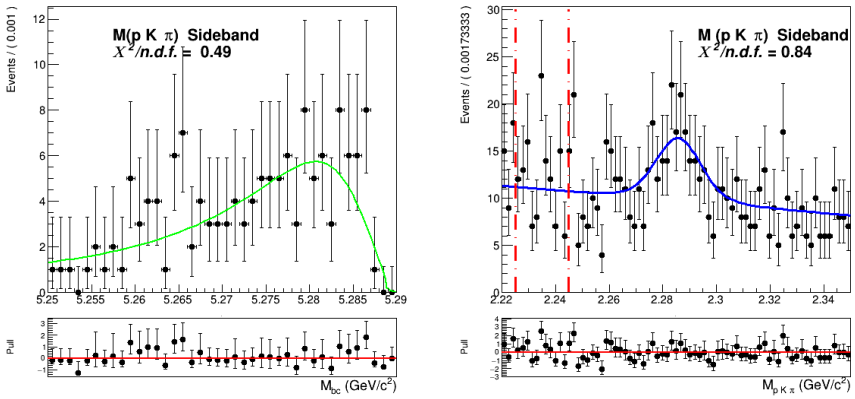

Figure (28) Two dimensional fit of crossfeed ($B^0\bar{B}^0$) events in M_{bc} and $M(pK\pi)$.

The procedure adopted to model the continuum background is the same used for the charged correlated $B \to \Lambda_c$ decays. To obtain the shape that can describe the continuum background M_{bc} distribution, the continuum suppression is not applied on the off-resonance continuum sample in order to acquire more statistics. It is then scaled and corrected for the *SignalProbability* correlated effects. The scaling and bin-correction procedure was carried out on a sample of five streams of on- and off-resonance MC. From a ratio plot, like the one in Fig. 29a, showing the continuum on-resonance distribution in M_{bc} and the scaled continuum on-resonance distribution without the continuum suppression applied, the bin-correction is obtained to correct the off-resonance data in the scaling procedure.

The validity of this procedure is first tested on the sixth independent MC sample: Fig. 29b shows the scaled and bin-corrected off-resonance continuum histogram compared with the continuum on-resonance distribution of the independent stream. Compared to the charged correlated decays one can notice larger statistical fluctuations but the overall result looks still fairly reasonable. In order to obtain the PDF describing the distribution the histogram is fitted (see Fig. 30a), i.e. with a Novosibirsk function.
Since in the Λ_c invariant mass one doesn't expect correlation effects, one can fit directly the properly scaled distribution with a first order polynomial (see Fig.30b) It is possible then to check the validity of the whole procedure on the on-resonance Monte Carlo independent stream (Fig. 31)

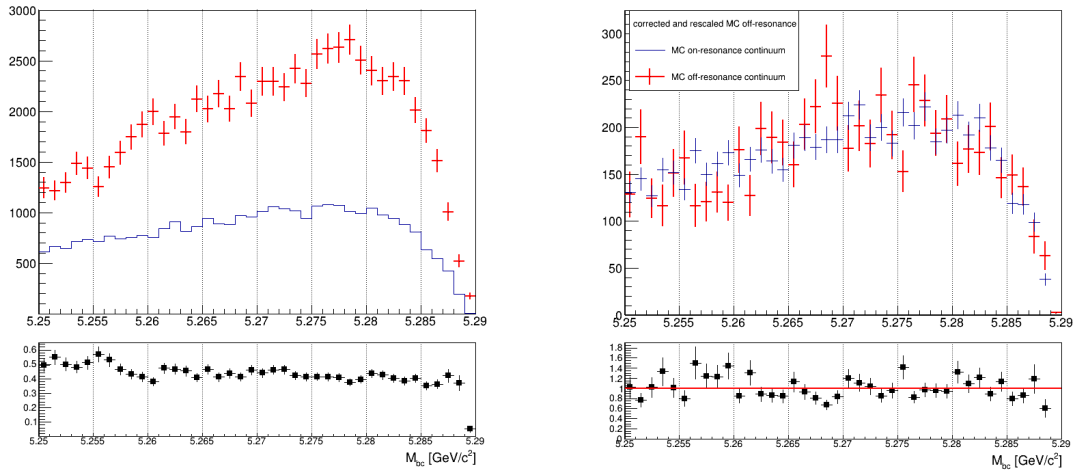

(a) (b)

Figure (29) On the left: M_{bc} distributions of the MC off-resonance sample without continuum suppression and the MC continuum sample with applied continuum suppression (5 streams). On the right: M_{bc} distributions of the corrected scaled MC off-resonance and on-resonance MC continuum (independent stream).

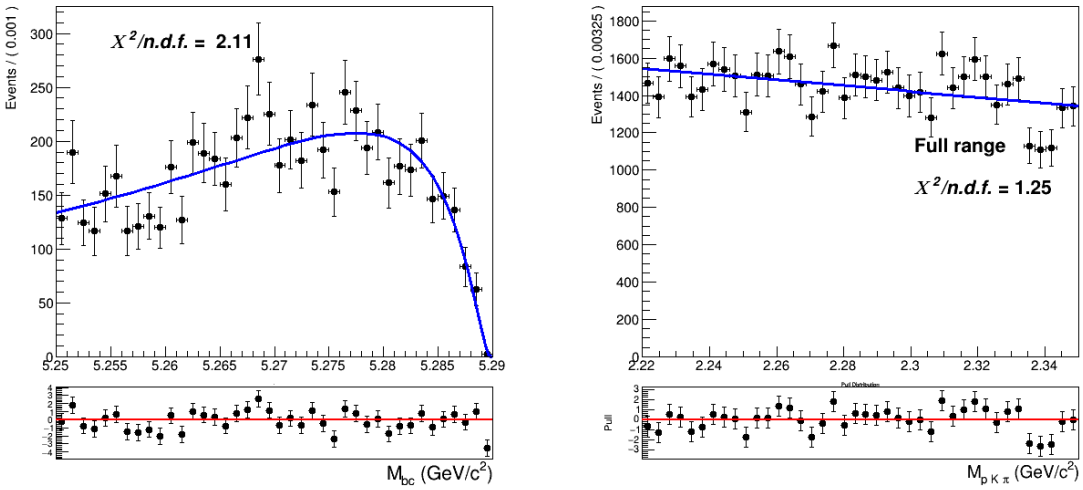

(a) (b)

Figure (30) On the left: fit of the M_{bc} distribution MC (scaled and corrected) off-resonance continuum (one stream). On the right: fit of the Λ_c invariant mass distribution of five stream scaled off-resonance continuum.

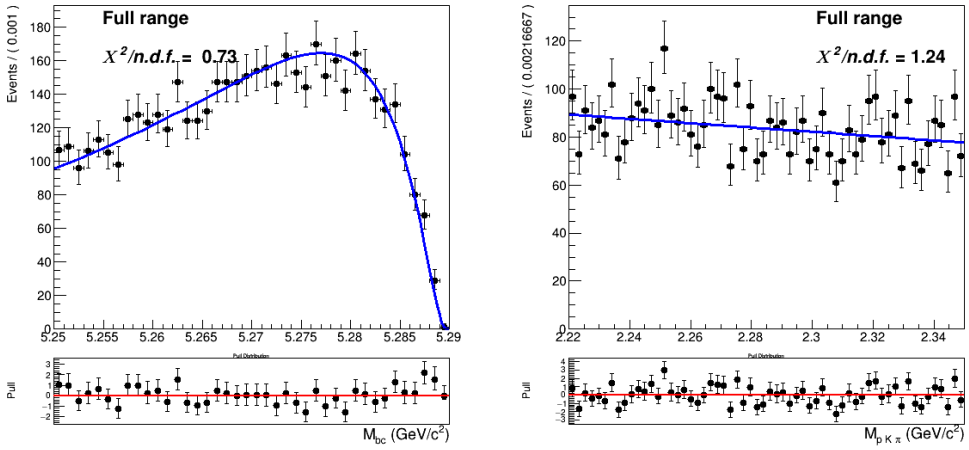

Figure (31) Continuum M_{bc} and $M(pK\pi)$ distributions overlaid by the PDFs obtained in fits shown in Figures 30a - 30b

5.2 Two dimensional fit

After obtaining the PDFs describing the various signal/background components using five streams statistics, the fit model is tested with six fits on the six independent Monte Carlo streams. The conditions for these six two dimensional fits are again the same used for the charged correlated decays (see Sec. **??**). Exemplary, the distributions of stream 0 overlaid

by the fitted PDF are depicted in Fig. 32 (see Appendix .3 for the projections in signal and sideband regions). In Table **??** the signal yields of the fits (**Reconstructed Signal**) to the two dimensional distributions for the six streams of $B^- \to \bar{\Lambda}_c^-$ flavor-anticorrelated decays are listed and compared to the expected yields of reconstructed signal, and fitted and truth-matched total signal events are also compared, together with their deviations.

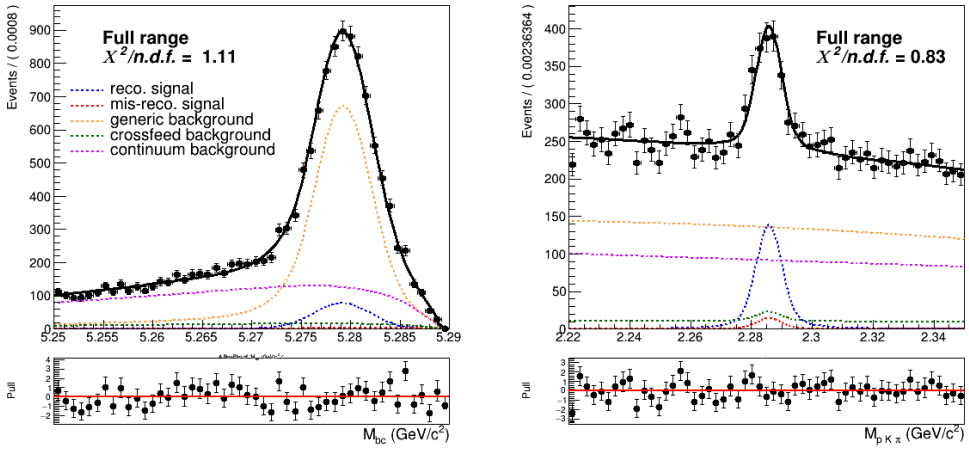

Figure (32) Two dimensional fit on stream 0 Monte Carlo simulated data.

	Reconstructed Signal		Total Signal			
	fit	expected	fit	MC truth	fit - MC truth	
stream 0	730 ± 60	660 ± 21	805 ± 65	765	40	5.2 %
stream 1	732 ± 60	698 ± 29	794 ± 63	785	9	1.1%
stream 2	759 ± 65	718 ± 29	800 ± 67	797	3	0.4%
stream 3	725 ± 58	702 ± 29	769 ± 60	802	-33	-4.1%
stream 4	829 ± 67	710 ± 29	944 ± 76	804	140	17.4%
stream 5	650 ± 61	675 ± 29	703 ± 62	760	-57	-8.1%
sum	4425	4163	4815	4718	102	+ 2.2%

Table (7) Comparison of fitted and expected signal yields, fitted and truth-matched total signal for six streams of Belle generic MC when fitting the two dimensional distributions of M_{bc} and $M(pK\pi)$.

Except for stream 4 all the fits show values of reconstructed signal within the 1σ uncertainties in agreement with the expected ones, but as already encountered in Sec. **??** a tendency of overestimation can be seen also in these fits, confirmed by the fit shown in Fig 34. Again this small, but not negligible, bias has to be taken into account while fitting the data.

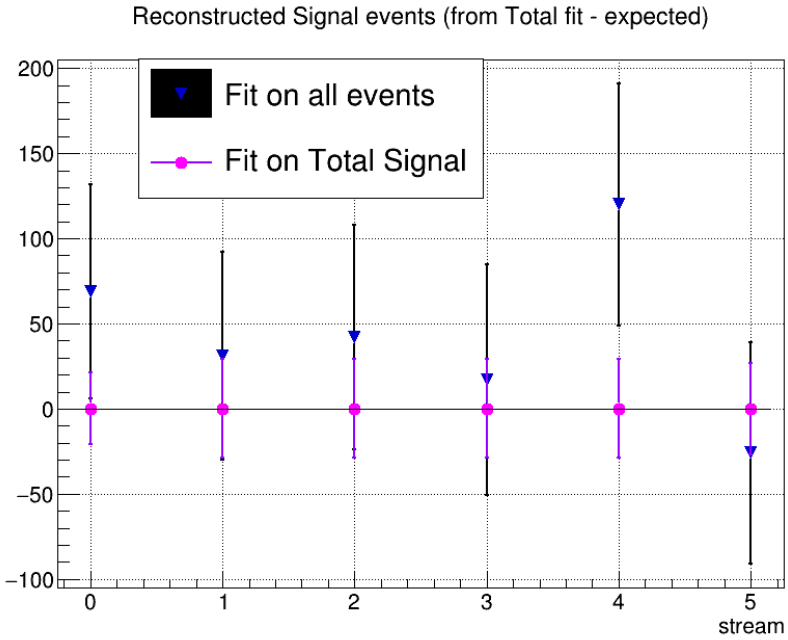

Figure (33) Differences between results from the fits and "expected" values for signal yields as reported in the first columns on Table 7 .

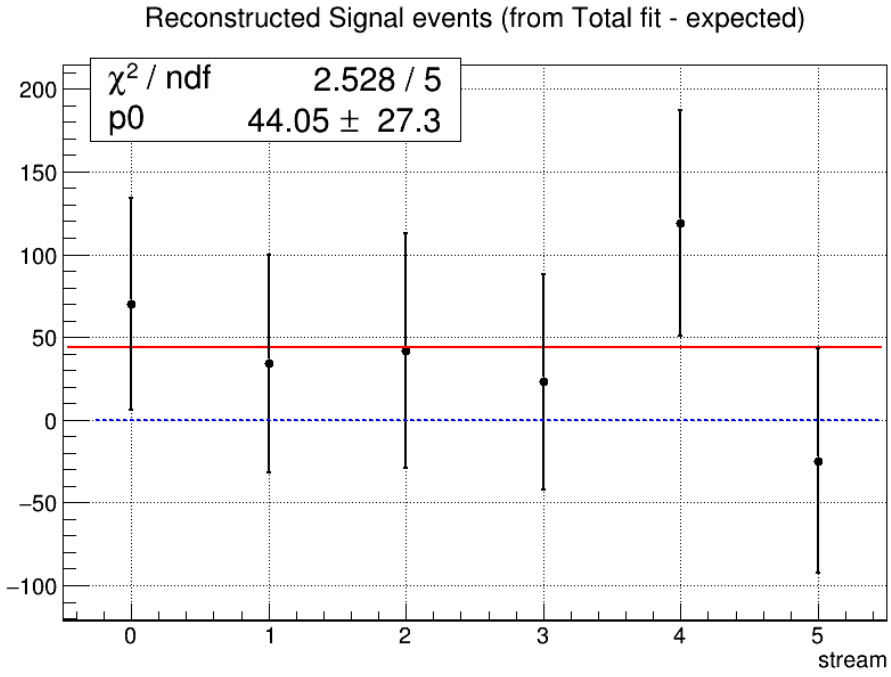

Figure (34)

389 Also the behaviour for different signal-to-background ratio was investigated using the six

independent streams of continuum and all the ten independent streams of $B\bar{B}$ events for the generic and crossfeed backgrounds and for the signal events. The amount of total signal is varied between 50% and 275% of the nominal (MC) values, in order to cover the values spanned by the uncertainties on the measurement perfromed by *BaBar* ($\mathcal{B}(B^+ \to \bar{\Lambda}_c^+ X) = 2.1^{+0.9}_{-0.6}$) and even the values covered by twice larger uncertainties as one can see in Fig. 36. The values seem to distribute according to a linear dependence, therefore also for this decay channel one doesn't expect any systematics due to different signal-to-background ratio.

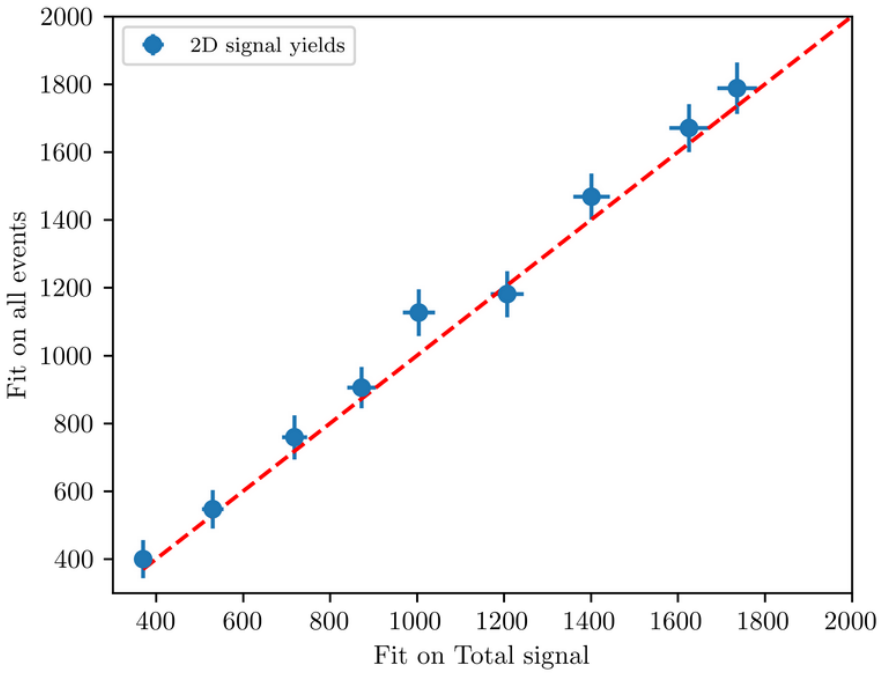

Figure (35) Linearity test: on the x-axis the obtained reconstructed signal yields from fits on different amounts of total signal; on y-axis the yields of reconstructed signal obtained fitting all events (as in Fig. **??**). The dashed red line represents the 1:1 linear dependence.

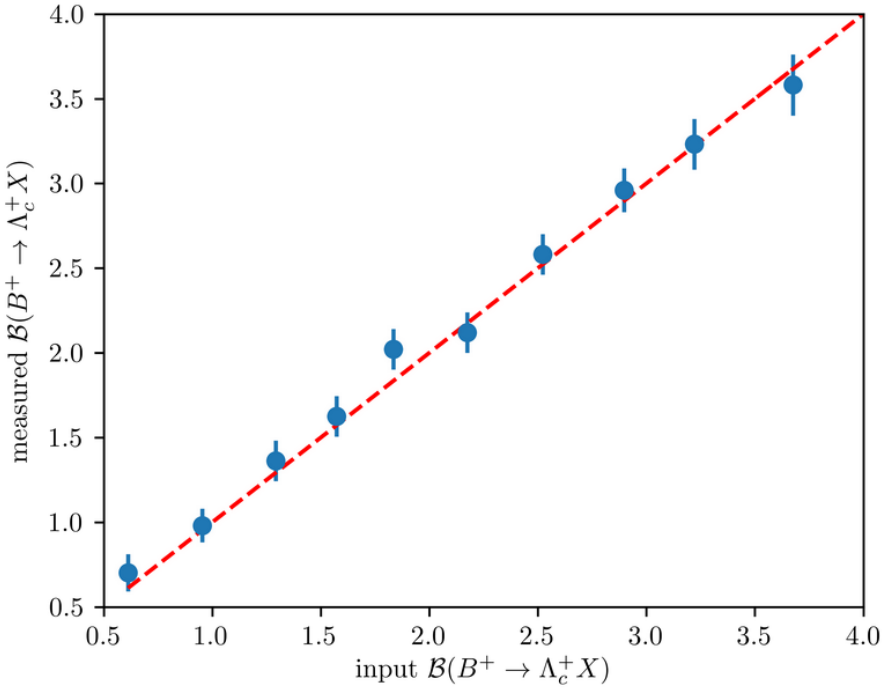

Figure (36) Linearity test: on the x-axis the input branching ratio value corresponding to the signal yields displayed on the x-axis in Fig. 35; on y-axis the measured branching fraction values corresponding to the signal yields of reconstructed signal displayed on the y-axis in Fig. 35.

Toy MC pseudo-experiments were performed as well (see Appendix).

5.3 Probability Density Functions (PDFs) for the B_{tag}

The M_{bc} distribution of the tagged B mesons is fitted with a Crystal Ball as for the "peaking" component and the "flat" component is fitted with a Argus function (Fig. 37a). The crossfeed background, consisting of neutral B mesons tagged as charged B, is fitted instead with a sum of a Novosibirsk and an asymmetric Gaussian PDF (Fig. 37b).

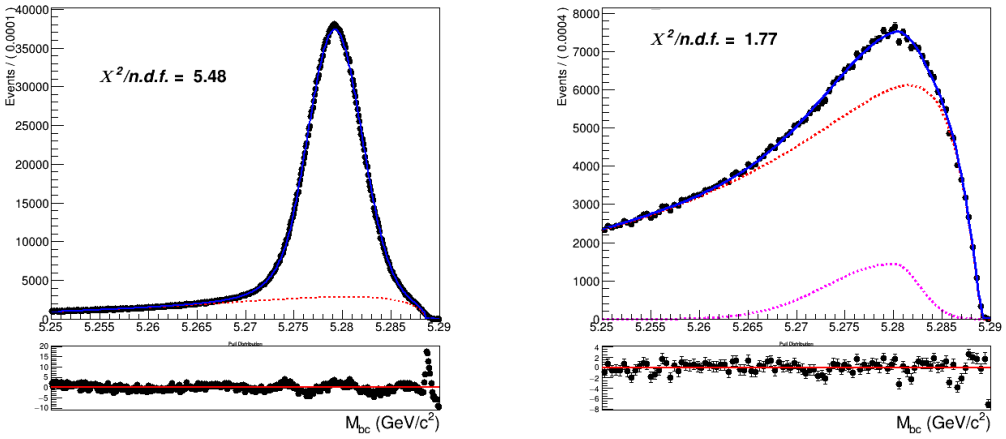

(a) (b)

Figure (37) On the left: fitted distribution of tagged charged B mesons, reconstructed signal events (magenta) are described by a Crystal Ball whereas the misreconstructed signal events (red) are described by an Argus function. On the right: Crossfeed distribution fitted with a sum of Novosibirsk (red) and asymmetric Gaussian PDF (magenta)

As for the continuum background, same procedure as the one in the case of charged flavor-correlated decays is adopted:

- first the off-resonance sample is scaled accordingly with all the included cuts.
- the ratio between the scaled off-resonance and the on-resonance in MC is calculated in each bin (see Fig. 38a)
- the bin-correction is applied on an independent stream and the scaled and bin-corrected M_{bc} distribution is compared with the on-resonance distribution as shown in Fig. 38b

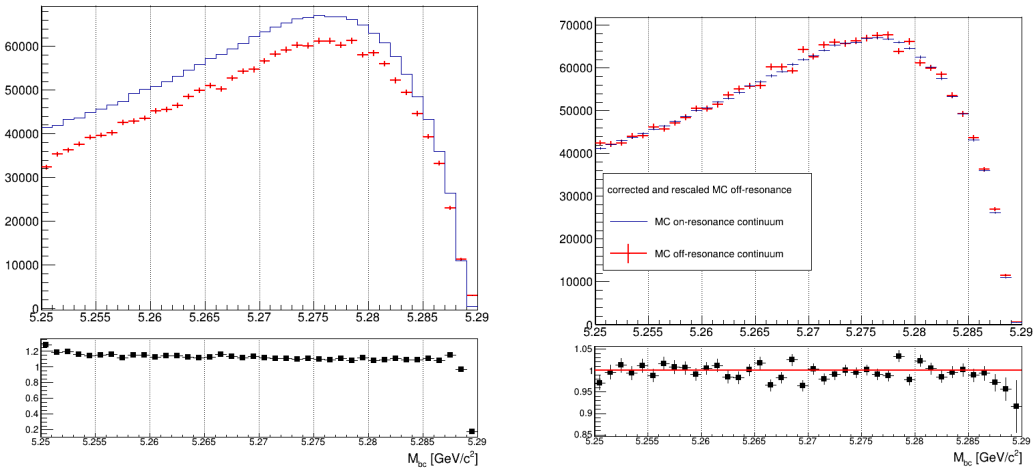

(a) (b)

Figure (38) On the left: M_{bc} distributions of the MC off-resonance sample and the MC continuum sample with applied continuum suppression. On the right: M_{bc} distributions of the corrected scaled MC off-resonance and on-resonance MC continuum.

5.4 B_{tag} fit

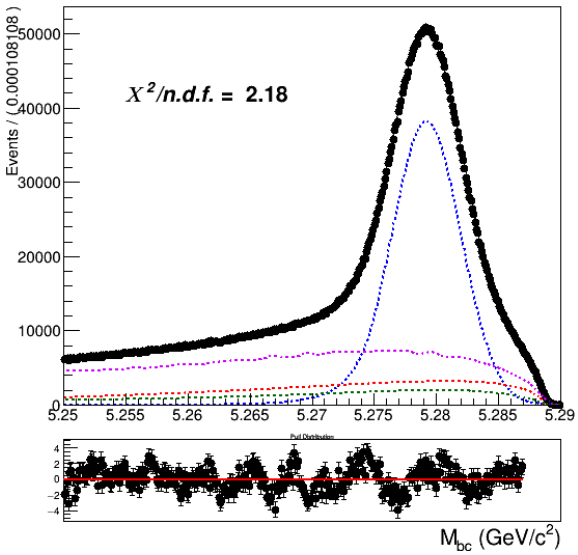

Figure (39) Total fit of tagged B mesons on Monte Carlo simulated data.

An independent Monte Carlo stream was used to test the total fit model on tagged B meson candidates. As in the 2D fit, the parameter for the width, σ_{CB}, of the Crystal Ball is floated and the ratio between expected crossfeed background events and misreconstructed signal events is fixed from the MC. The Argus function describing the misreconstructed signal is also not fully constrained: the parameter describing the tail is free. As in the previous B_{tag} fits, the range for the fit is restricted to values betweeen 5.250 and 5.287 GeV/c^2. Yields for the reconstructed and misreconstructed signal are obtained from the fit:

NrecSig	$2.5099 \cdot 10^6 \pm$ 4408
NmisSig	$7.82307 \cdot 10^5 \pm$ 2936

The Total Signal (the sum NrecSig+NmisSig) is 3292168 ± 2423 (to be compared with 3299629 from the Monte Carlo), which means a $\sim 3\sigma$ underestimation. As in the case of charged flavor-correlated decays, this can produce some systematic effect which needs to be taken into account. In fact, a slight underestimation of the Total Signal is found also in the result of the toy Monte Carlo study[4]: Fig. 40 shows the results for the Total Signal events and one can notice a mean value for the pulls consistently below zero.

[4] as usual performed with 3×10^3 pseudo-datasets

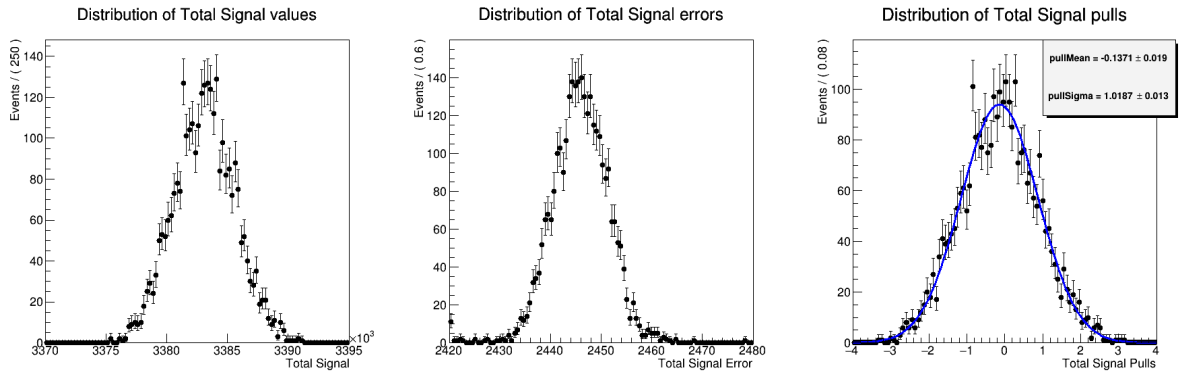

Figure (40) Toy MC fits of pseudo-data showing the Total Signal yield (left), Total Signal yield errors (center) and the pull distribution of the Total Signal (right).

5.5 Λ_c and FEI efficiency

The efficiency in reconstructing the Λ_c baryon after correctly tagging the charged B meson, is as usual estimated as the ratio:

$$\frac{N_{recSig}(B_{tag}, \Lambda_c)}{N_{recSig}(B_{tag}^{sig})} \tag{3}$$

where $N_{recSig}(B_{tag}, \Lambda_c))$ are the yields of reconstructed signal from the two dimensional fits (reported in Table 7) and $N_{recSig}(B_{tag}^{sig})$ are the yields of correctly reconstructed signal in a fit of B mesons tagged in events where one of the two mesons decayed hadronically and inclusively into a Λ_c baryon (see Fig **??**). This ratio was calculated upon six streams of Monte Carlo simulated data.

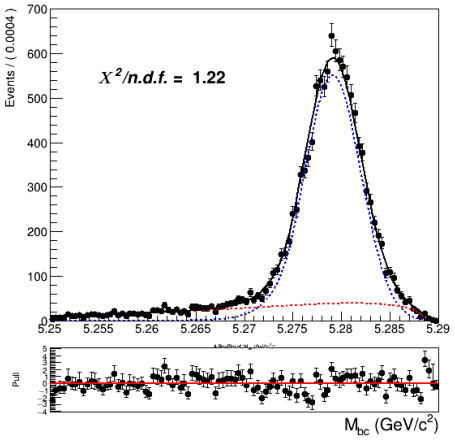

Figure (41) Fit of tagged B mesons in the "signal events" sample

From this and the results listed in Sec. 5.2 the efficiency to reconstruct Λ_c is obtained :

$\epsilon_{\Lambda_c} = \frac{NrecSig(B_{tag},\Lambda_c)}{NrecSig(N_{recSig}(B_{tag}} = 40.95 \pm 1.77\%$

The yields from the fit shown in Fig. 41) are then used to calculate the FEI tag-side efficiency for signal events. The yields from the fit of charged B_{tag} shown in Fig. 37a can be used to calculate the hadronic tag-side efficiency in the generic B^+B^- events case.

The ratio between the two efficiencies is calculated: $\frac{\epsilon^+_{FEI,sig}}{\epsilon^+_{FEI}} = 0.973 \pm 0.009$

5.6 Studies of Systematic Effects

The systematic uncertainties are estimated the same way as in the case of charged flavor-correlated decays (see **??** and the following Sections). In Table 8 the systematic uncertainties of the various considered sources are summarized. Their individual calculation is outlined in the subsequent subsections (the uncertainties on the PID efficiency corrections are the same already discussed in **??**)

source	%
Continuum modeling	0.04
Crossfeed PDFs	0.01
Crossfeed fraction	0.01
2DFit crossfeed normalization	0.01
2DFit crossfeed peaking fraction	0.08*
$\epsilon^+_{FEI,sig}/\epsilon^+_{FEI}$	0.01
ϵ_{Λ_c}	0.05
Fit bias	0.05
PID	0.02
Tracking efficiency	0.01
Total	0.12

Table (8) Systematic uncertainties in the determination of the $B^- \to \bar{\Lambda}_c^- X$ branching fractions in %.

* as in the case of charged flavor-correlated decays this uncertainty can be possibly reduced with a new measurement of $B^0 \to \Lambda_c$ decays.

5.7 Continuum background modeling

Exemplary, fits used to estimate the impact of these uncertainties deriving from statistical uncertainties are shown here in Figures 42 - 43. Mean deviation values are then obtained for both the two-dimensional fit and the B_{tag} fit.

Fit	$-\sigma$	$+\sigma$	$\pm\bar{\sigma}$
2D	21	22	22
B_{tag}	5800	5800	5800

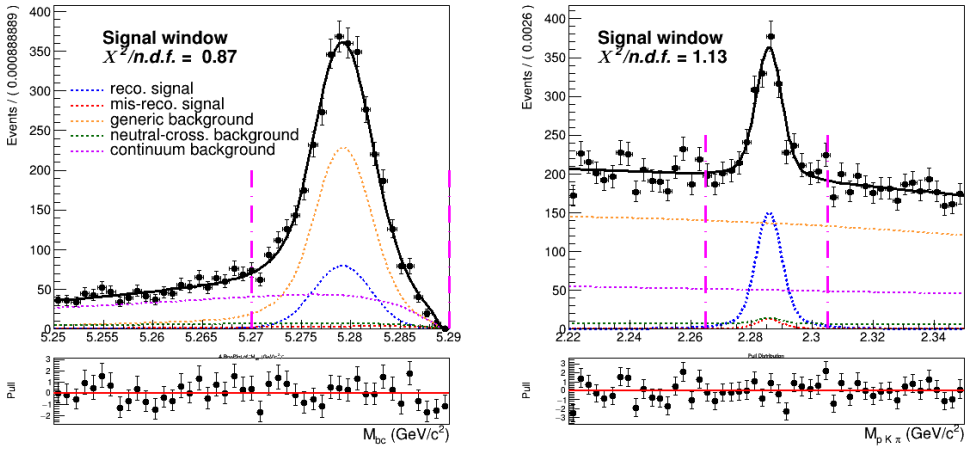

Figure (42) Signal window projections of a two dimensional fit on Monte Carlo simulated data where the shaping parameters were varied of their uncertainties.

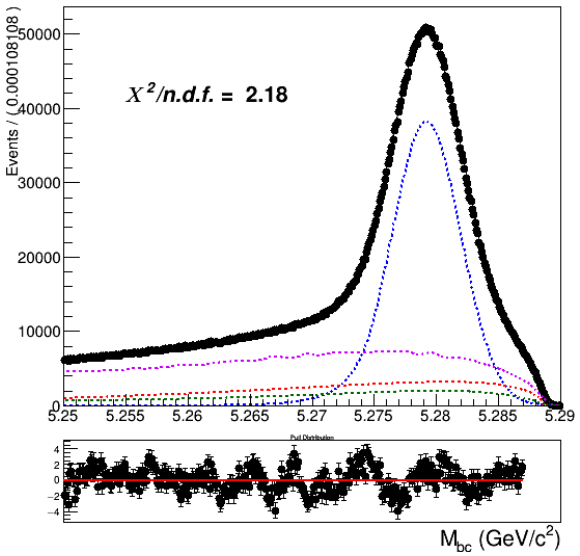

Figure (43) Fit of tagged B meson candidates on Monte Carlo simulated data where the shaping parameters were varied of their uncertainties.

The estimated systematic uncertainty on Br value from this source is 0.04%.

The continuum suppression cut is found to reject about 68% of the continuum background in data, whereas it rejects 64% of the continuum background in MC (66.5% in

on-resonance MC). This means that in data one can expect about 1.4% less continuum background events. The statistical uncertainty on this fraction of events can be also be taken into account as systematics. But again, as already seen in the case of charged flavor-correlated decays, the statistical uncertainty on the on-resonance continuum background events in MC originates a much larger systematic uncertainty: the relative systematic uncertainty deriving from the different impact on data of the continuum suppression would account for just 0.004% on the BR value (one order of magnitude smaller than systematics deriving from the statistical uncertainties). This second source is again consequently neglected.

5.8 Crossfeed background modeling

This source of systematic uncertainty is again estimated performing the fits varying the parameters of the Crossfeed PDFs by their uncertainties (see the table below for the deviations in terms of signal yields). The resulting absolute systematic uncertainty is about 0.006% on the BR value, which is rounded up to 0.01%.

Fit	$-\sigma$	$+\sigma$	$\pm\bar{\sigma}$
2D	3	3	3
B_{tag}	1500	1100	1300

Table (9) Offsets on the signal yields obtained varying the parameters of crossfeed background PDFs within their uncertainties in the two dimensional and B_{tag} fit and mean deviations reported in the last column.

5.9 Crossfeed ratio

As already done for the charged flavor-correlated decays, the systematic uncertainty on the crossfeed/misreconstructed signal "probability ratio" for the 2D fit and cross-feed/misreconstructed ratio is studied considering a maximal discrepancy up to 20% between Monte Carlo and data (the procedure adopted is the same as illustrated in **??**).

Fit	$-\sigma$	$+\sigma$	$\pm\bar{\sigma}$
2D	4	8	6
B_{tag}	5800	800	3300

Table (10) Offsets on the signal yields obtained varying of $\pm 20\%$ the k ratio in the two dimensional and B_{tag} fit and mean deviations reported in the last column.

The estimated systematic uncertainty on Br value from this source is 0.01%.

5.10 Parametrization of crossfeed normalization in the 2D fit

The statistical uncertainties on the parameters used in the parametrization of crossfeed normalization in the 2D fit are estimated to originate a systematic uncertainty of 0.01% on the Br value.

5.11 Crossfeed peaking fraction in the 2D fit

As already done for the charged correlated decays, to estimate this systematic uncertainty the amount of crossfeed events peaking in $M(pK\pi)$ was varied in order to cover the uncertainties on the branching fraction for neutral decays and the two-dimensional fit repeated with those values. The difference in signal yields obtained is reported in the following table.

Fit	$-\sigma$	$+\sigma$	$\pm\bar{\sigma}$
2D	15	18	16

Table (11) Offsets on the signal yields obtained varying the amount of peaking crossfeed in the Λ_c invariant mass and mean deviation.

The uncertainity originated is estimated to be of 0.08% on the Br value.

5.12 Efficiencies

The ratio between the two FEI efficiencies is: $\frac{\epsilon^+_{FEI,sig}}{\epsilon^+_{FEI}} = 0.973 \pm 0.009$
The uncertainity on this value originates a systematic uncertainty of 0.01% on the Br value. The Λ_c reconstruction efficiency is determined to be $\epsilon_{\Lambda_c} = 40.95 \pm 1.77\%$. When propagating its uncertainty, a systematic error of 0.07% on the Br value is calculated.

5.13 Fit biases

The small bias on the reconstructed signal seen in the two-dimensional fit model produces a not negligible systematic uncertainty on the branching fraction. The discrepancy in the amount of the total signal estimated by the B_{tag} fit needs to be included as well in the systematic effects. Propagating the two sources of systematics in the branching fraction calculation results in an additional 0.05% uncertainty on the branching fraction value.

5.14 Tracking efficiency

As for the charged correlated decays, a systematic uncertainty of 0.35% per track is applied and the total systematic uncertainty is the sum over the three charged tracks used to reconstruct the Λ_c baryon: 1.05%. This results in 0.01% uncertainty on the branching fraction value.

5.15 Measured $B^+ \to {\Lambda_c}^+$ inclusive Branching Fraction

Using the results from the two dimensional fit reported in Table 7 with all the needed factors known, it's possible to examine the agreement between the the branching ratio value used in MC generation and the measured ones. As in the charged flavor-correlated decays the average of measured values are about 1σ statistical uncertainty away from the average value of the branching ratio set in MC (actually already the average value obtained with the total signal fits shows this tendency).

	total fit	signal fit	BELLE MC VALUE
stream 0	$(1.32 \pm 0.11)\%$	$(1.19 \pm 0.04)\%$	$(1.233 \pm 0.007)\%$
stream 1	$(1.32 \pm 0.11)\%$	$(1.26 \pm 0.05)\%$	$(1.218 \pm 0.007)\%$
stream 2	$(1.37 \pm 0.12)\%$	$(1.29 \pm 0.05)\%$	$(1.218 \pm 0.007)\%$
stream 3	$(1.31 \pm 0.11)\%$	$(1.26 \pm 0.05)\%$	$(1.215 \pm 0.007)\%$
stream 4	$(1.50 \pm 0.12)\%$	$(1.26 \pm 0.05)\%$	$(1.218 \pm 0.007)\%$
stream 5	$(1.12 \pm 0.12)\%$	$(1.22 \pm 0.05)\%$	$(1.217 \pm 0.007)\%$
average	$(1.32 \pm 0.05)\%$	$(1.25 \pm 0.02)\%$	$(1.220 \pm 0.003)\%$

Table (12) Measured branching fraction values obtained using the results listed in Table 7 for the six different streams (only statistical uncertainties are displayed) and its average.

As in the charged flavor-correlated decays the precision obtained on Monte Carlo simulated data is improved by factors compared to the branching fraction measured by BaBar experiment (see [1]).

Appendices

.1 $B^- \to \Lambda_c^+$ decays: additional plots

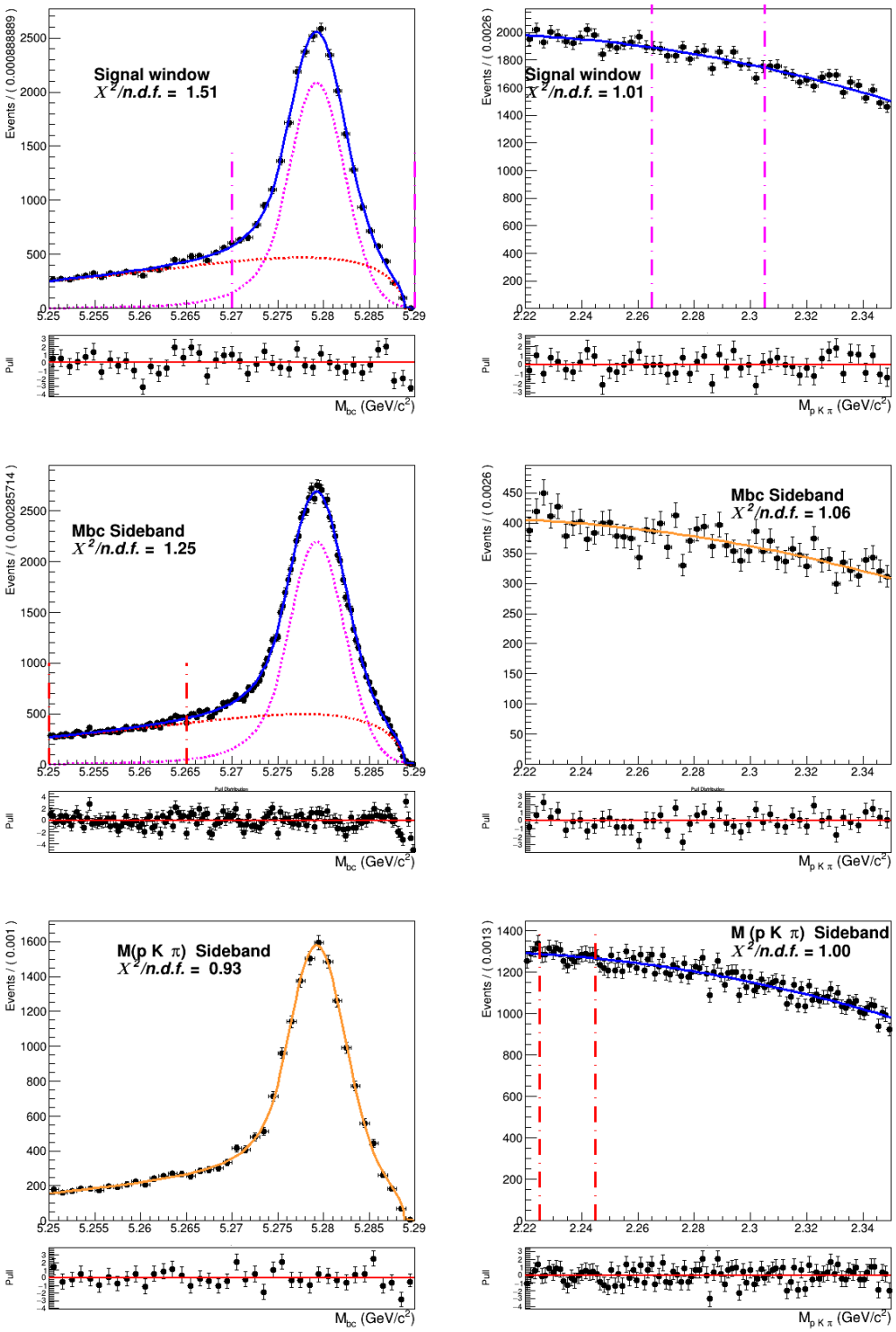

Figure (44) Signal region and sidebands of the two dimensional fit of generic background shown in **??**

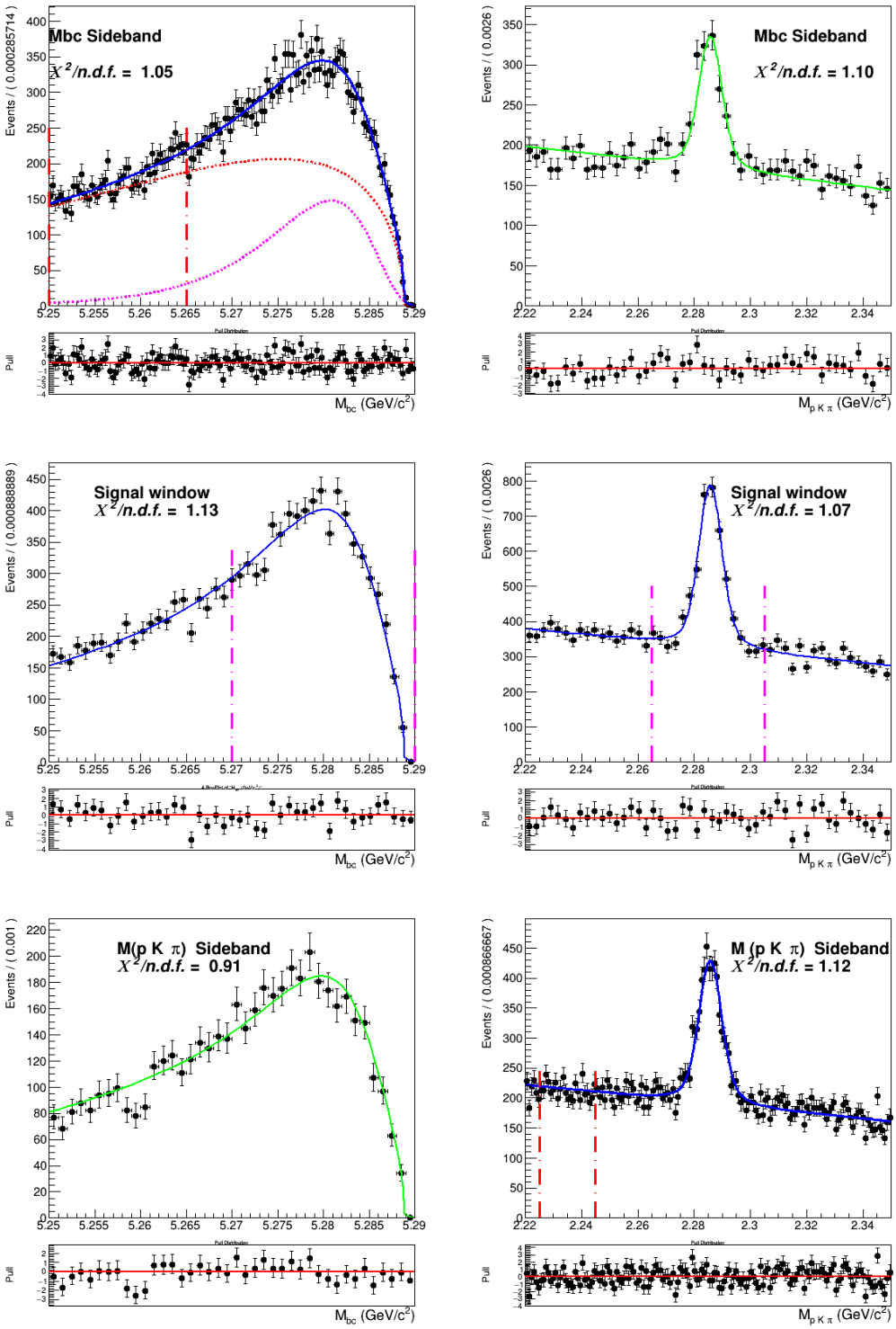

Figure (45) Signal region and sidebands of the two dimensional fit of crossfeed background after parametrization

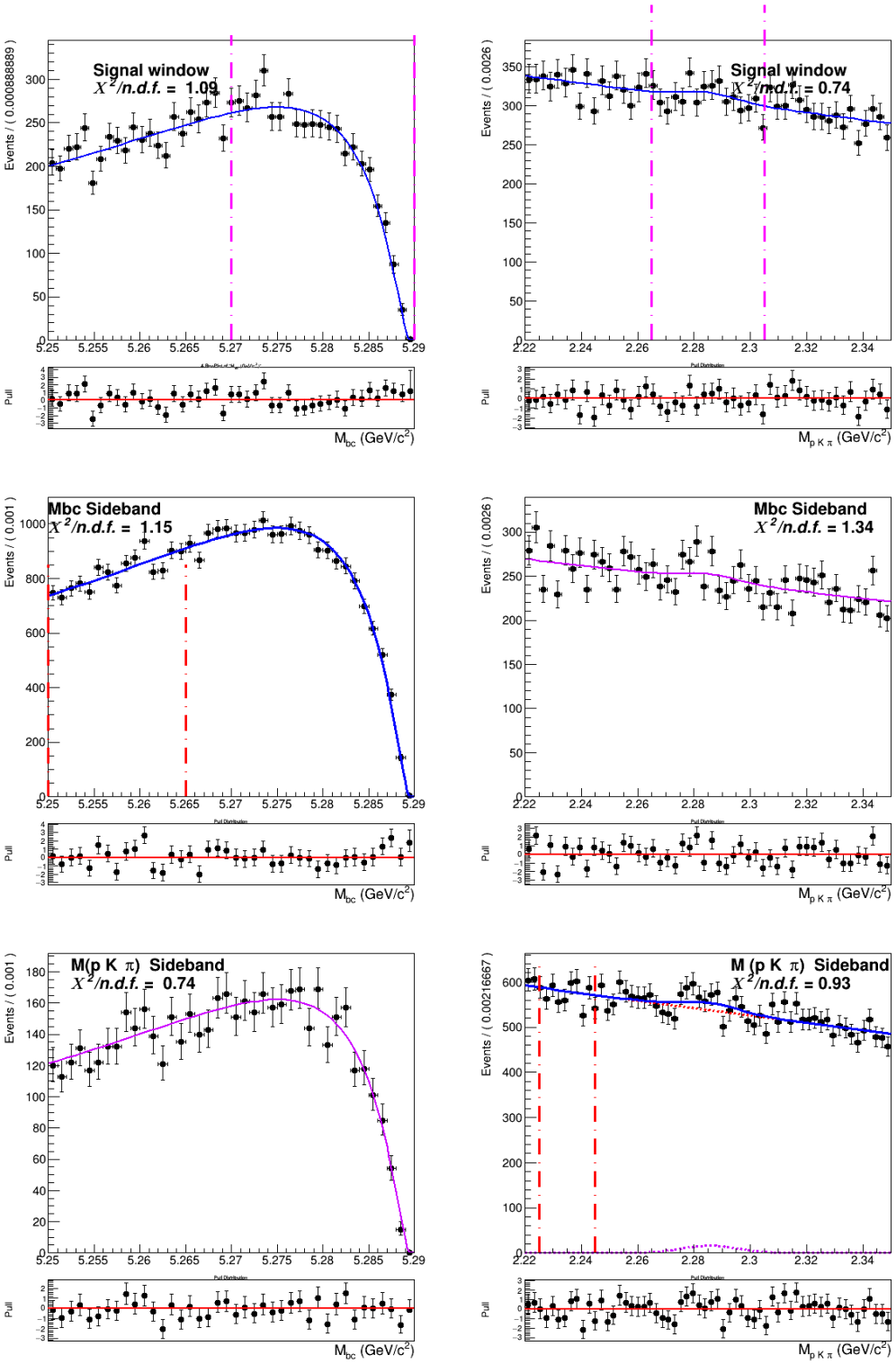

Figure (46) Signal region and sidebands of the two dimensional fit of continuum background shown in ??

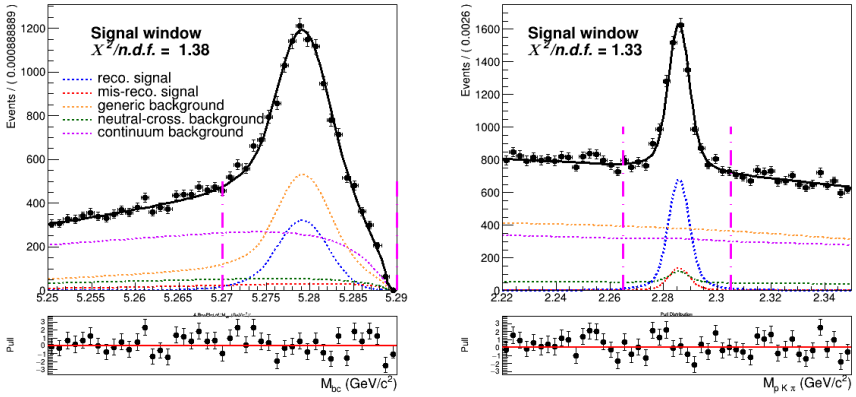

Figure (47) Signal region ($2.22 < M(pK\pi) < 2.35$ GeV/c^2 and $5.27 < M_{bc} < 5.29$ GeV/c^2) projections pf the dimensional fit on stream 0 Monte Carlo simulated data.

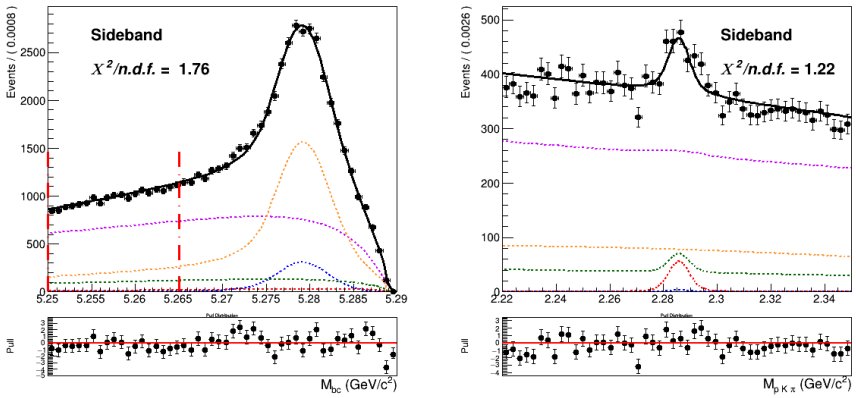

Figure (48) Sideband region of $5.25 < M_{bc} < 5.265$ GeV/c^2 projection of the two dimensional fit on stream 0 Monte Carlo simulated data.

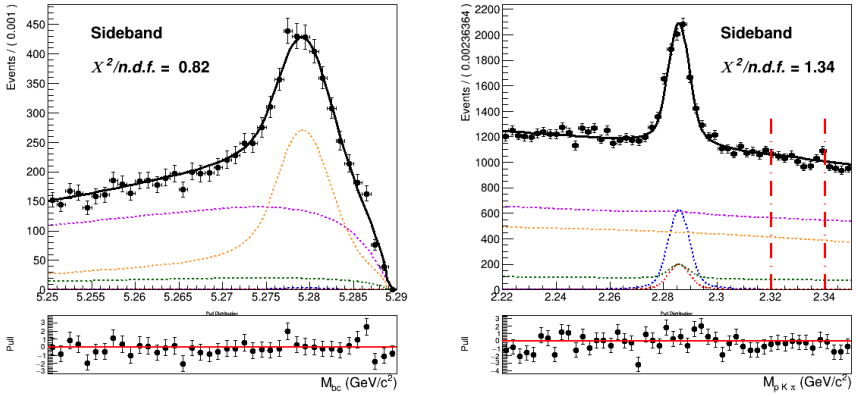

Figure (49) Sideband region of $2.22 < M(pK\pi) < 2.35$ GeV/c^2 projection of the two dimensional fit on stream 0 Monte Carlo simulated data.

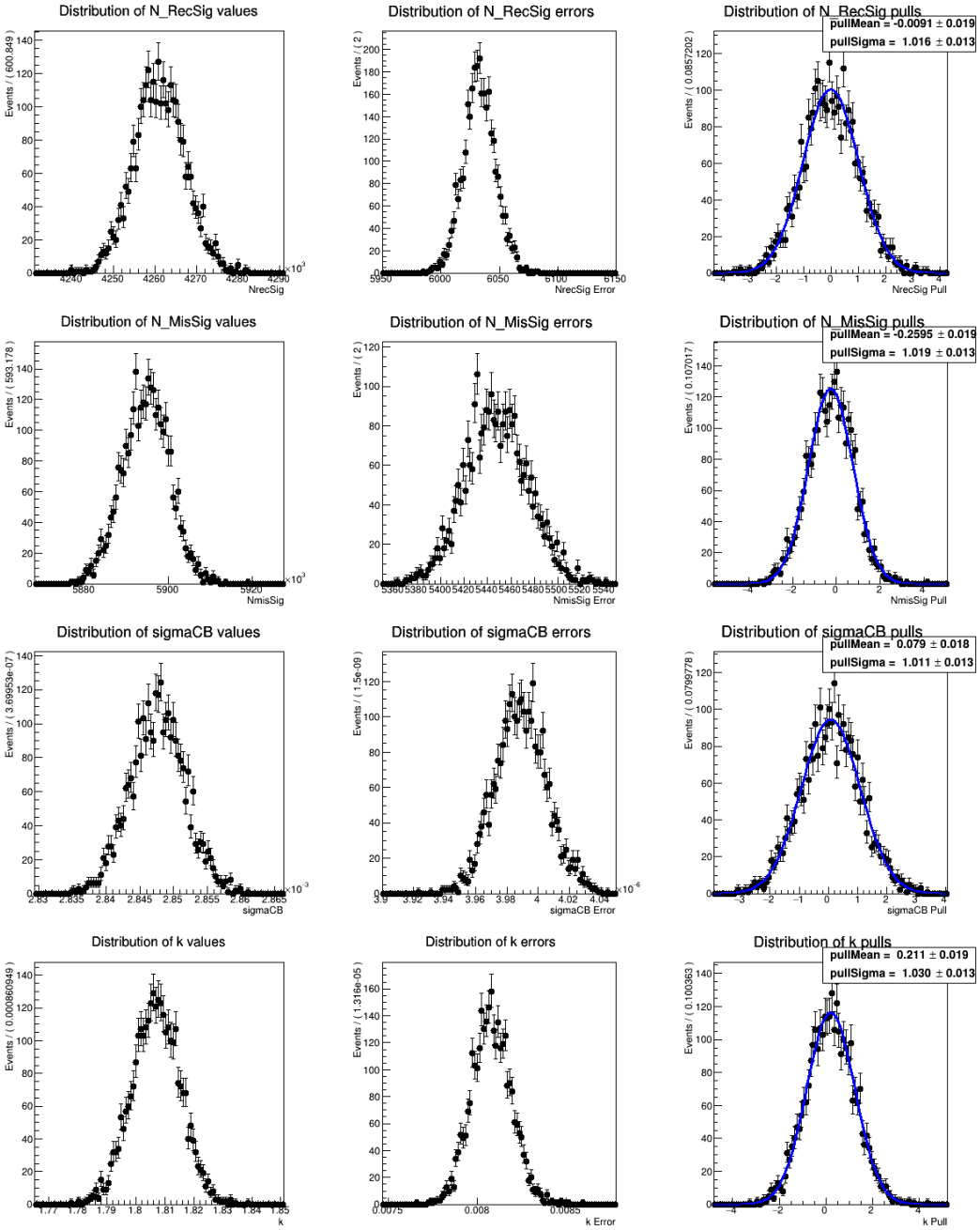

Figure (50) Toy MC study for the B_{tag} fit model described in Sec. **??**

.2 $B^- \to D^0$ decays: additional plots

Figures 51-52 show the FOM values at various cuts on $foxWolframR2$ and SignalProbability variables respectively. After the cuts on the first two variables were optimized, the cut on D^0_{CMS} is chosen considering the momenta distributions plotted on 53: $p^{D^0}_{CMS} > 1$ GeV/c^2 removes a good portion of background events while retaining most of the signal events.

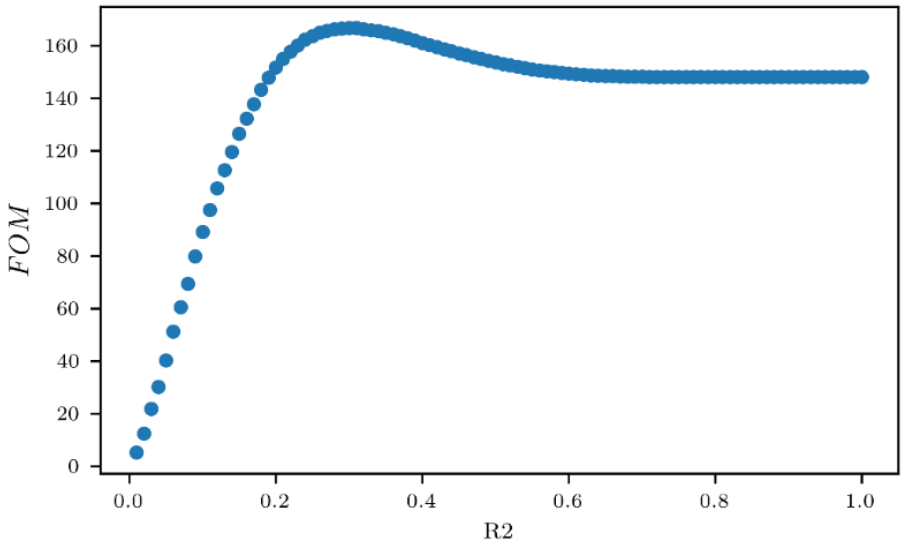

Figure (51) Figure of Merit values calculated at several cuts on the $foxWolframR2$ variable.

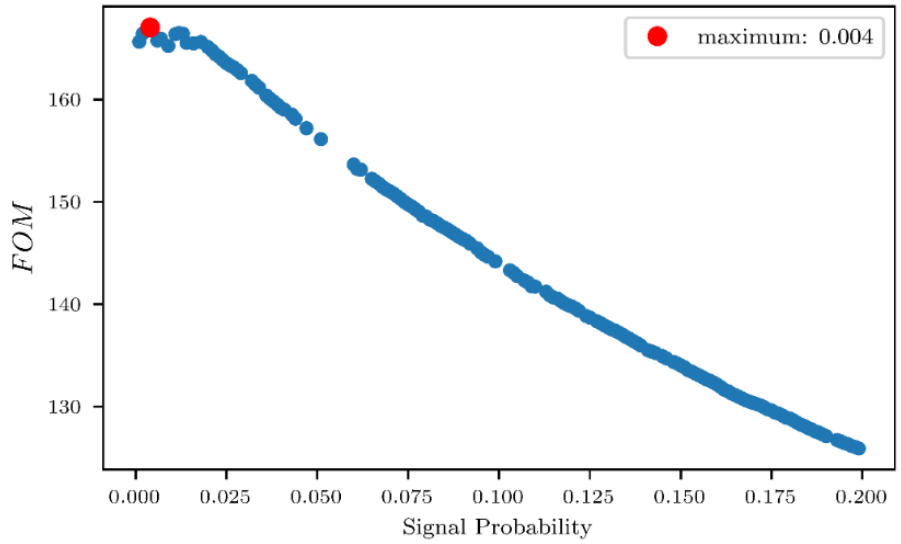

Figure (52) Figure of Merit values calculated at several cuts on the SignalProbability variable.

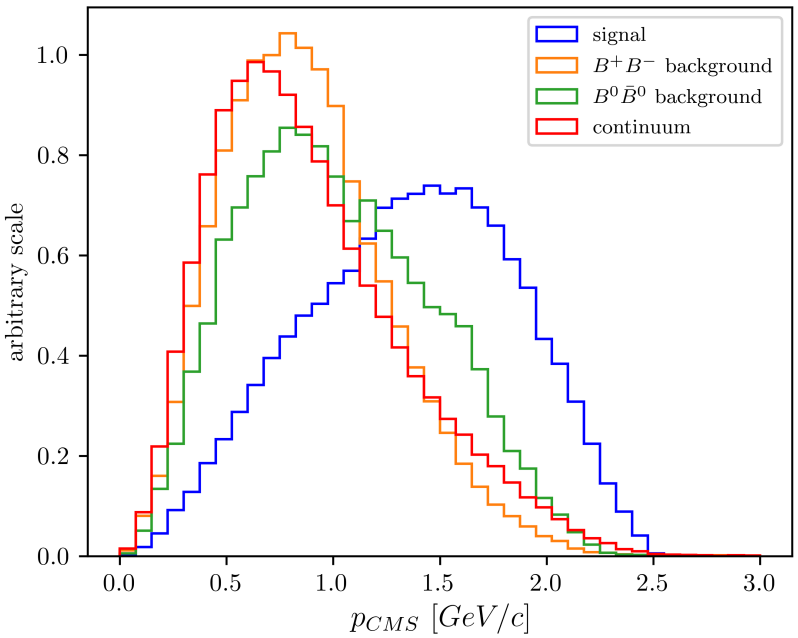

Figure (53) Distribution of D^0 candidates momenta in the center of mass system after the cuts on $foxWolframR2$ and SignalProbability variables were applied.

Figures 54-56 show the projections of signal regions and sidebands in M_{bc} and in the D^0 invariant mass of the two dimensional fit on stream 0.

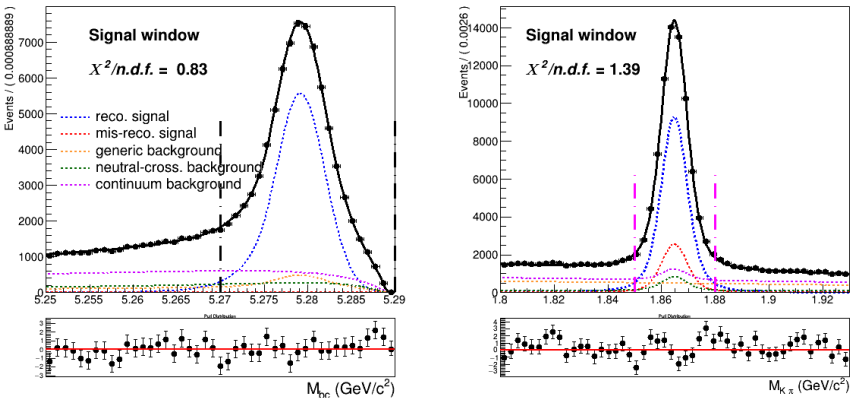

Figure (54) Signal region ($1.85 < M(\pi K) < 1.88$ GeV/c^2 and $5.27 < M_{bc} < 5.29$ GeV/c^2) projections of the two dimensional fit on stream0 (Fig. 10).

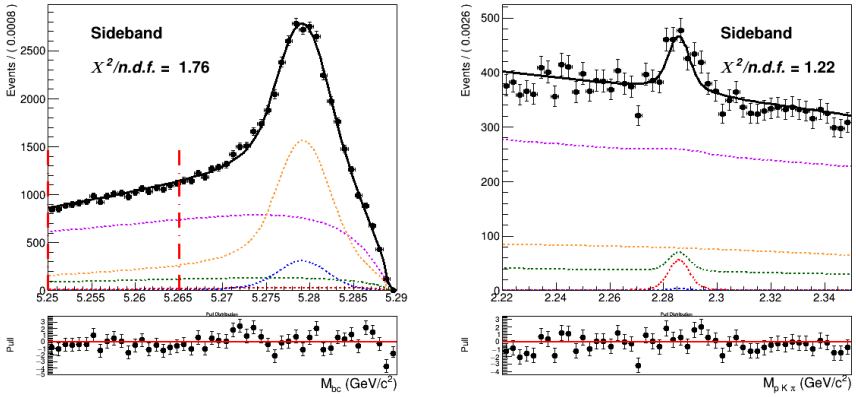

Figure (55) Sideband region of $5.25 < M_{bc} < 5.265$ GeV/c^2 projection in $M(\pi K)$ of the two dimensional fit on stream 0.

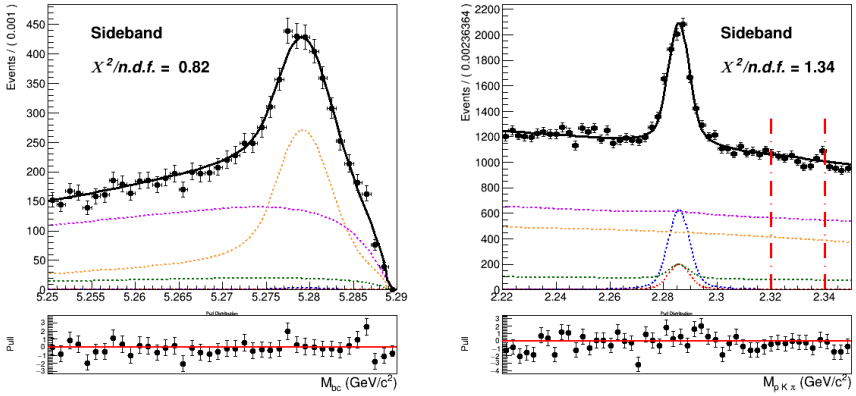

Figure (56) Sideband region of $1.8 < M(\pi K) < 1.84$ GeV/c^2 projection in M_{bc} of the two dimensional fit on stream 0.

Figs. 57 to 59 show the projections in M_{bc} and in the D^0 invariant mass of the two dimensional fit on data.

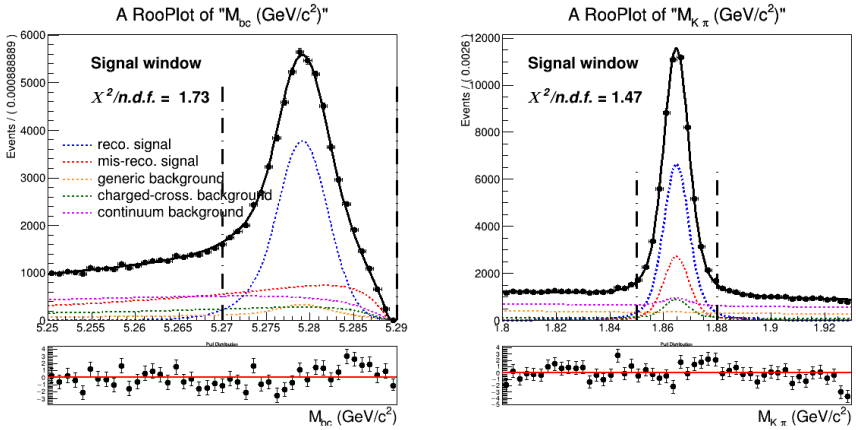

Figure (57) Signal region ($1.85 < M(\pi K) < 1.88$ GeV/c^2 and $5.27 < M_{bc} < 5.29$ GeV/c^2) projections of the two dimensional fit on data described in Sec. 4.6

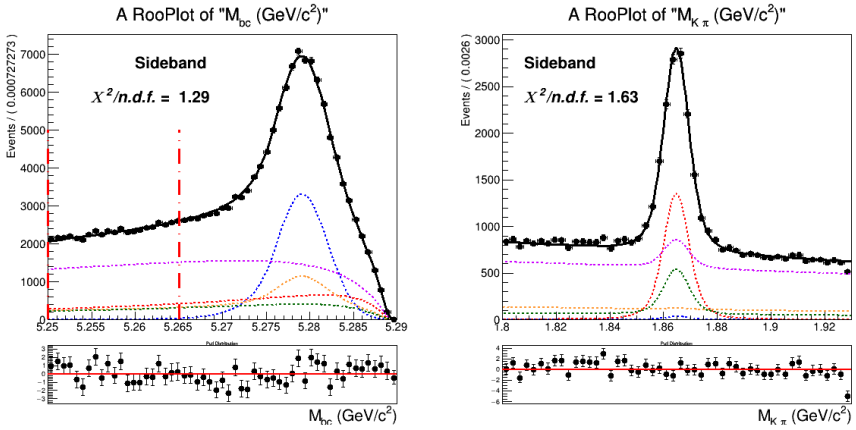

Figure (58) Sideband region of $5.25 < M_{bc} < 5.265$ GeV/c^2 projection in $M(\pi K)$ of the two dimensional fit on data

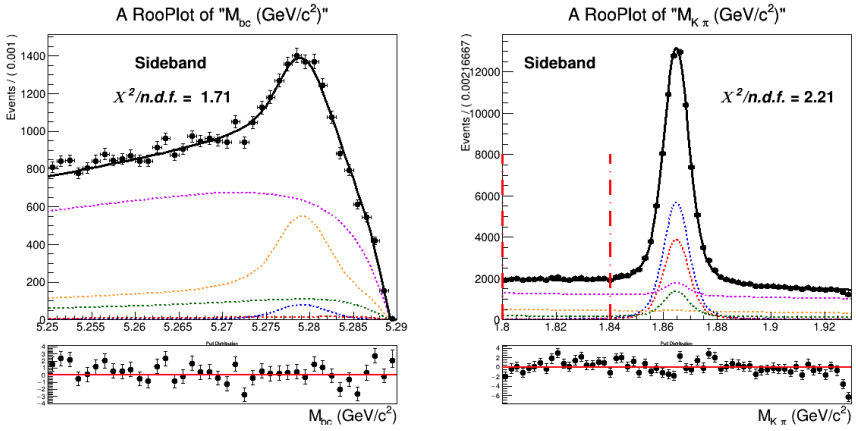

Figure (59) Sideband region of $1.8 < M(\pi K) < 1.84$ GeV/c^2 projection in M_{bc} of the two dimensional fit on data.

.3 $B^- \to \bar{\Lambda}_c^-$ decays: additional plots

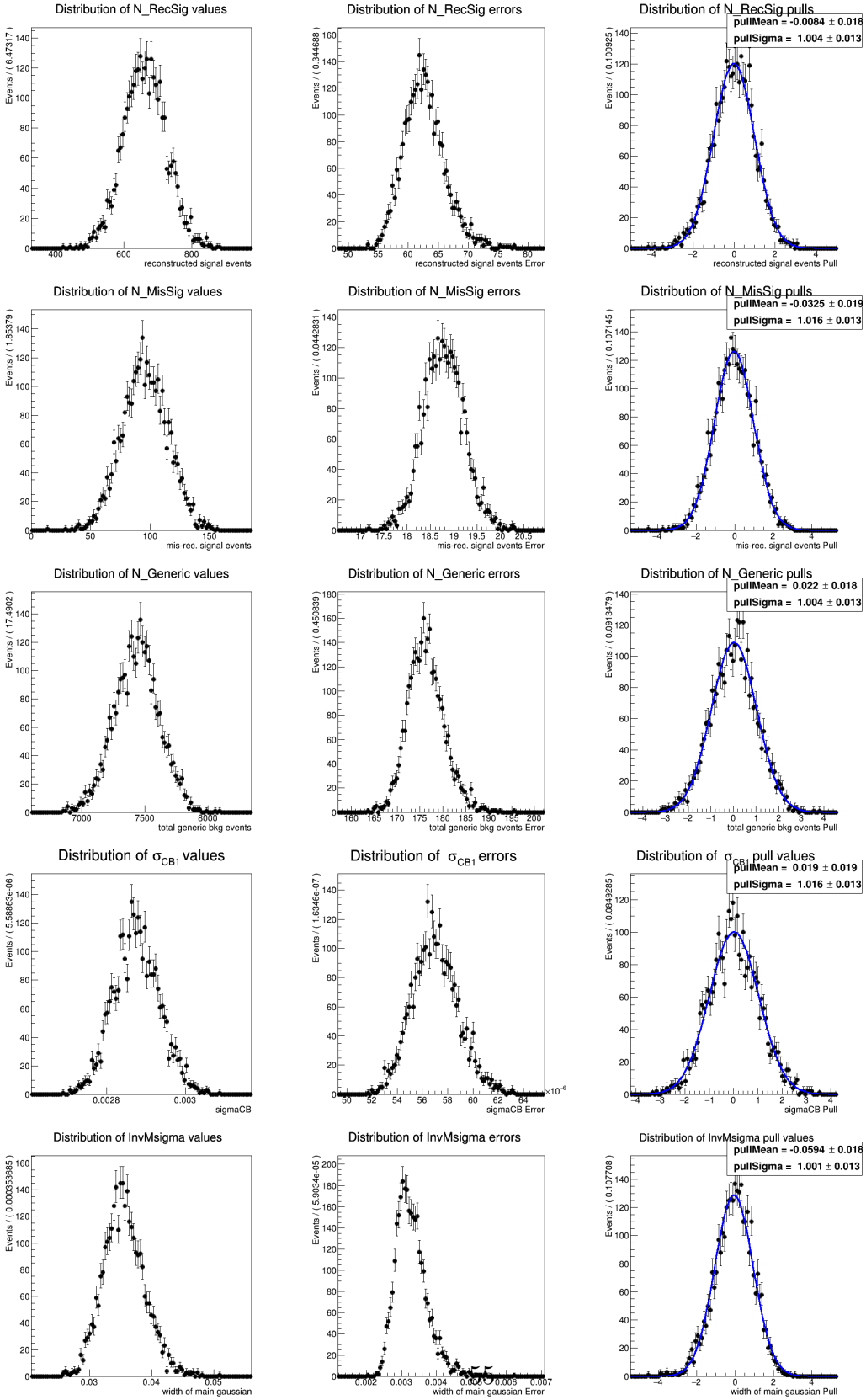

Figure (60) Toy MC study for the two dimensional fit model described in Sec. 5.2

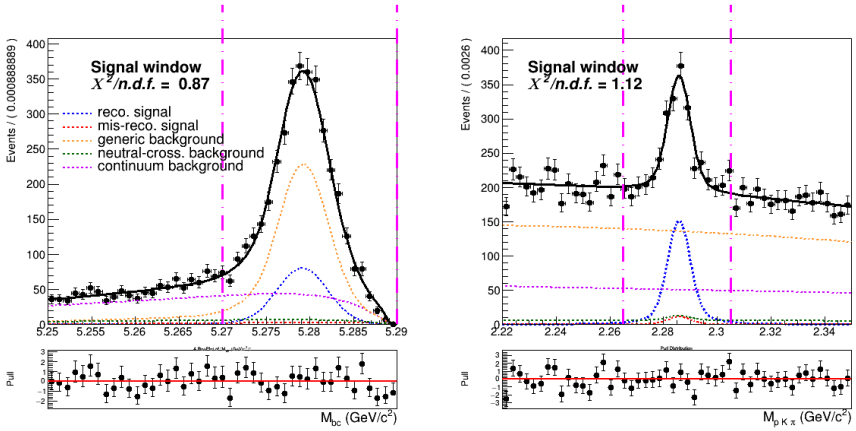

Figure (61) Signal region ($2.22 < M(pK\pi) < 2.35$ GeV/c^2 and $5.27 < M_{bc} < 5.29$ GeV/c^2) projections of the dimensional fit on stream 0 Monte Carlo simulated data.

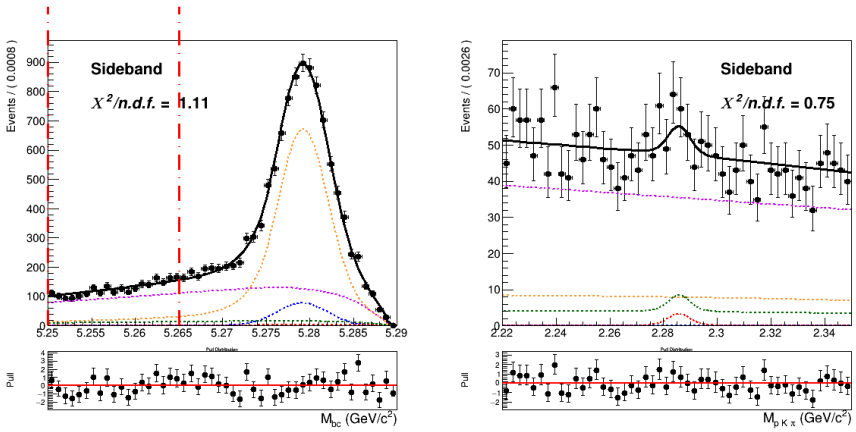

Figure (62) Sideband region of $5.25 < M_{bc} < 5.265$ GeV/c^2 projection of the two dimensional fit on stream 0 Monte Carlo simulated data.

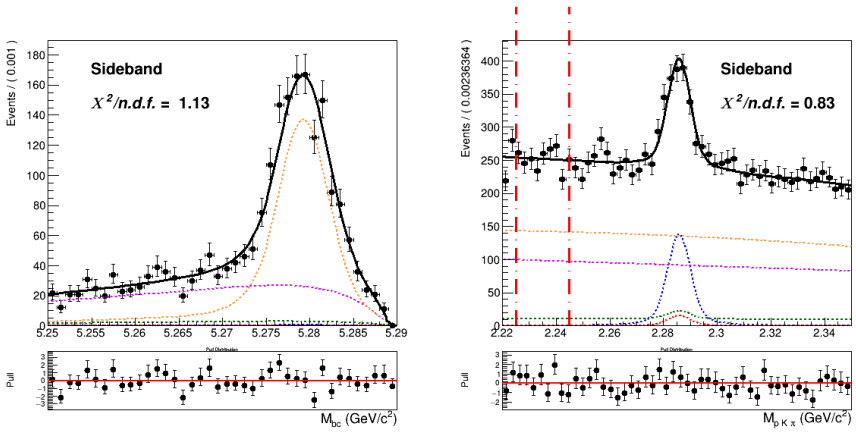

Figure (63) Sideband region of $2.22 < M(pK\pi) < 2.35$ GeV/c^2 projection of the two dimensional fit on stream 0 Monte Carlo simulated data.

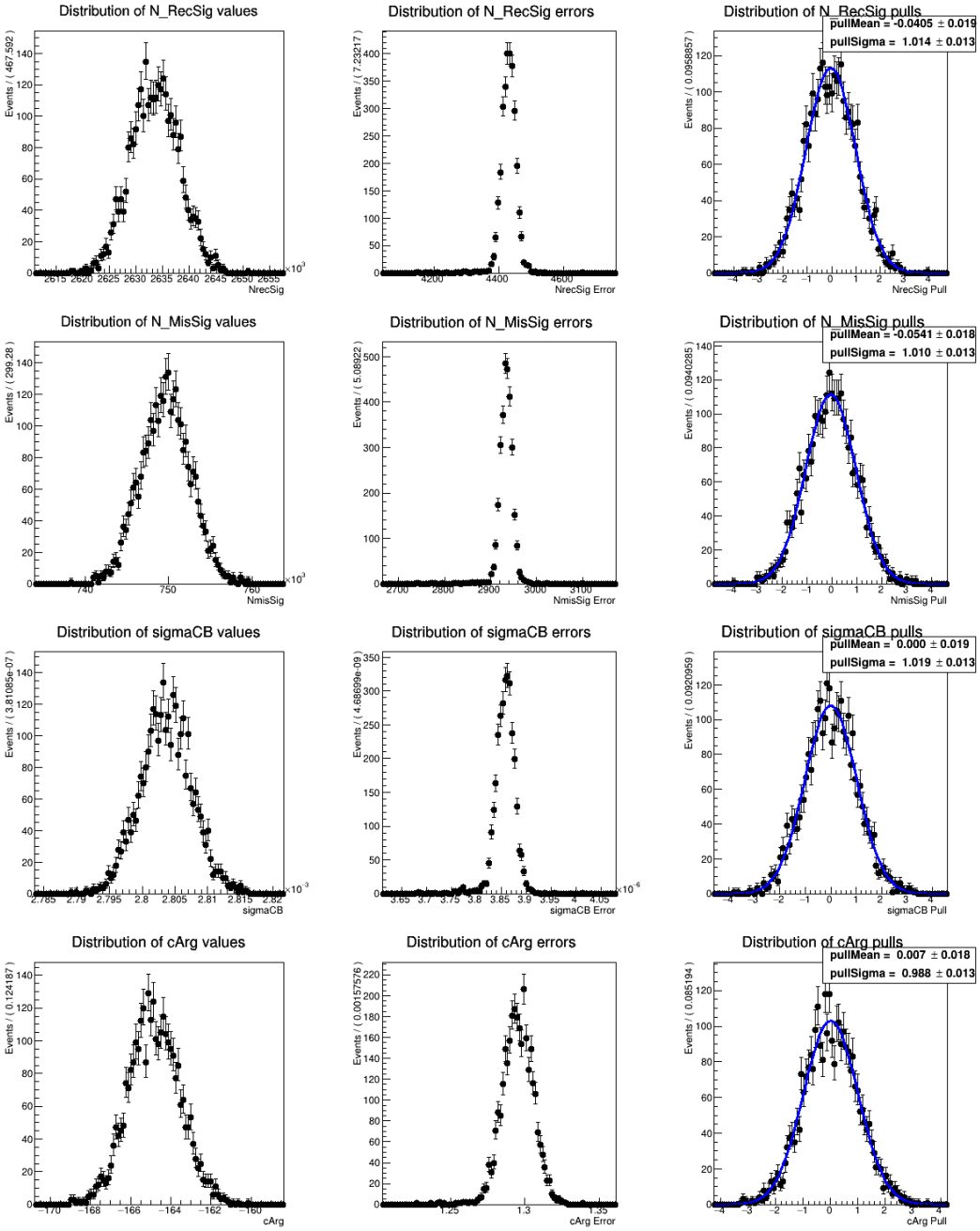

Figure (64) Toy MC study for the B_{tag} fit model described in Sec. 5.4

References

[1] B. Aubert et al., BaBar, *Study of inclusive B^- and $\bar{B}^0$ decays to flavor-tagged D, D_s and Λ_c^+*, Phys. Rev. D **75** (2007) 072002, arXiv:hep-ex/0606026.

[2] I. Grach, I. Narodetskii, S. Simula, and K. Ter-Martirosyan, *Exclusive and inclusive weak decays of the B-meson*, Nuclear Physics B **502** (1997) no. 1-2, 227–248.

[3] Y. Hsiao, S.-Y. Tsai, C.-C. Lih, and E. Rodrigues, *Testing the W-exchange mechanism with two-body baryonic B decays*, Journal of High Energy Physics **2020** (apr, 2020) . https://doi.org/10.1007/JHEP04(2020)035.

[4] M. Gelb, *Search for the Rare Decay* $\mathrm{B}^+ \to \ell^+ \nu_\ell \gamma$ *with the Full Event Interpretation at the Belle Experiment*. PhD thesis, Karlsruhe Institute of Technology (KIT), 2018.

[5] J. Schwab, *Calibration of the Full Event Interpretation for the Belle and the Belle II Experiment*, Master's thesis, Karlsruhe Institute of Technology (KIT), 2017.

[6] K.-J. Tien and M.-Z. Wang, *Proton identification efficiency study*, BELLE NOTE 1279.

[7] S. Nishida, *Study of Kaon and Pion Identification Using Inclusive D^* Sample*, BELLE NOTE 779.

[8] B. Bhuyan, *High P_T Tracking Efficiency Using Partially Reconstructed D^* Decays*, BELLE NOTE 1165.
https://belle.kek.jp/secured/belle_note/gn1165/BN1165_v1.pdf.

[9] C. H. e. a. B. Fulsom, *Search for $B^0 \to \Lambda^0 \Psi_{DM}$ decays*, BELLE NOTE 1584.
https://belle.kek.jp/secured/belle_note/gn1584/BN1584_v1.pdf.